The Rare Neurocutaneous Disorders

Update on Clinical, Molecular, and Neuroimaging Features

Felipe S. Barros, MD,[*] Victor Hugo R. Marussi, MD,[*] Lázaro L.F. Amaral, MD,[*] Antônio José da Rocha, MD, PhD,[†] Christiane M.S. Campos, MD,[*] Leonardo F. Freitas, MD,[*] Thierry A.G.M. Huisman, MD,[‡] and Bruno P. Soares, MD[‡]

Abstract: Phakomatoses, also known as neurocutaneous disorders, comprise a vast number of entities that predominantly affect structures originated from the ectoderm such as the central nervous system and the skin, but also the mesoderm, particularly the vascular system. Extensive literature exists about the most common phakomatoses, namely neurofibromatosis, tuberous sclerosis, von Hippel-Lindau and Sturge-Weber syndrome. However, recent developments in the understanding of the molecular underpinnings of less common phakomatoses have sparked interest in these disorders. In this article, we review the clinical features, current pathogenesis, and modern neuroimaging findings of melanophakomatoses, vascular phakomatoses, and other rare neurocutaneous syndromes that may also include tissue overgrowth or neoplastic predisposition.

Key Words: brain MRI, hemimegalencephaly, incontinentia pigmenti, magnetic resonance imaging, melanosis, mTOR, neurocutaneous disorders, PHACES syndrome, phakomatosis, phosphatase and tensin homolog, vascular malformation

(*Top Magn Reson Imaging* 2018;27:433–462)

Neurocutaneous disorders, also known as phakomatoses, classically refer to a group of diseases that features abnormalities involving predominantly structures originating from the ectoderm such as the central nervous system (CNS) and the skin, but also the vascular system given its common origin from the neural crest. The term phakomatosis, first described in 1920, comes from the Greek word for birthmark, which accurately correlates with the clinical hallmark of these disorders: skin changes.

The CNS and the skin share common developmental origins. The development of the CNS begins at 2 to 3 weeks of gestation when the neural plate appears as a thickened layer of ectoderm at the cranial dorsal midline of the embryo. The neural plate forms the neural tube by the process of primary neurulation, in which thickening and infolding of the neural plate with subsequent fusion at the midline creates the neural tube while separating from the overlying closing cutaneous ectoderm.[1,2] The molecular signals for primary neurulation include sonic hedgehog (SHH), WNT, and bone morphogenetic protein (BMP) signaling pathways.[3–5]

TEACHING POINTS

- Phakomatoses comprise a large number of entities that predominantly affect structures originated from the ectoderm (central nervous system and skin) and mesoderm (vascular system), classically divided into 3 different subgroups, listed as melanophakomatoses, vascular, and other phakomatoses.
- Melanophakomatoses include a variety of entities including cutaneous lesions ranging from hypo- to hyperpigmented skin abnormalities. The most common entities are hypomelanosis of Ito and incontinentia pigmenti.
- Hypomelanosis of Ito usually presents with a distinctive pattern of the skin involvement, which is characterized by hypomacular zones with irregular borders, ''V'' or ''S'' shaped, striations, swirls, patches, or whorls along the lines of Blaschko, typically not associated with inflammatory changes. Imaging findings include T2/FLAIR white matter abnormalities in association with cystic lesions/prominent perivascular spaces within the white matter of the parietal lobes.
- Incontinentia Pigmenti usually presents with hyperpigmented skin lesions along the lines of Blaschko and are classically associated with inflammatory changes. The most common imaging features are brain infarctions and T2/FLAIR white matter signal abnormalities; however, hemorrhagic lesions along with ischemic changes have been reported. Patchy punctate lesions with restricted diffusion along the cerebral and cerebellar hemispheres add specificity to the diagnosis.
- Vascular phakomatoses include a variety of entities in which the cutaneous lesions are present in association with low-flow or high-flow vascular abnormalities of both the skin and the central nervous system. The most common entities are Ataxia Telangiectasia and Rendu-Osler-Weber disease. Spinal and cerebral metameric syndromes are also subgroups of vascular phakomatoses.
- Ataxia Telangiectasia is the most common cause of cerebellar ataxia in children younger than 5 years of age and the second most common pediatric neurodegenerative disorder involving the cerebellum. It presents classically with ocular abnormalities, visual impairment, and oculocutaneous telangiectasias. Affected patients most commonly presents with diffuse progressive cerebellar atrophy.
- Rendu-Osler-Weber disease is a highly penetrant autosomal vascular neurocutaneous disorder. Its hallmark is the presence of multiples arteriovenous malformations (AVMs) involving many organs and tissues, such as central nervous system, lungs, and gastrointestinal tract. The most common symptom is anemia due to the chronic gastrointestinal bleeding, however, severe pulmonary hemorrhage due to pulmonary AVMs is a major cause of death. Neuroimaging findings include several small cerebral AVMs, which tend to occur superficially and have a low Spetzler-Martin grade.
- Other phakomatoses include a miscellaneous group of entities that most commonly present as overgrowth syndromes with a higher risk of tumorigenesis, such as Proteus syndrome and basal nevus syndrome.

After the closure of the neural tube, cells at the neural crest will give origin to both structures derived from ectoderm and mesoderm (eg, blood vessels and melanocytes). Several genes are related to promotion of neural crest differentiation, such as *PAX3*, *BMP4*, *WNT1*, *EGR2*, *SOX10*, among others. Abnormal differentiation of the neural crest constitute the basis for several neurocutaneous disorders and their remarkable association between brain, skin, and vascular abnormalities.[6]

From the [*]Division of Neuroradiology, BP Medicina Diagnóstica, Hospital da Beneficência Portuguesa de São Paulo; [†]Division of Neuroradiology, Department of Radiology, Santa Casa de São Paulo School of Medical Sciences, São Paulo, Brazil; and [‡]Division of Pediatric Radiology and Pediatric Neuroradiology, Russell H. Morgan Department of Radiology and Radiological Science, Johns Hopkins University School of Medicine, Baltimore, MD.

Address correspondence to Bruno P. Soares, MD, Division of Pediatric Radiology and Pediatric Neuroradiology, Russell H. Morgan Department of Radiology and Radiological Science, Johns Hopkins University School of Medicine, 1800 Orleans St, Zayed Tower, Rm 4174, Baltimore, MD 21287 (e-mail: bruno.soares@jhmi.edu).

DOI: 10.1097/RMR.0000000000000185

Melanoblasts are derived from the neural crest and later differentiate into melanocytes. They migrate to the dermal-epidermal junction to produce melanin. However, arrested migration with persistence of melanocytes in the dermis may lead to skin abnormalities such as Mongolian spot, cellular blue nevus, nevus of Ito, and nevus of Ota (NO).[7] Arrested migration of melanoblasts from the neural crest may also result in pigmentary abnormalities involving the brain, meninges, inner ear, eye, and nerve fibers.[7]

In this article, we review clinical features, molecular basis and pathophysiology, and imaging findings of less common neurocutaneous disorders. According to their embryologic origin and main affected tissues, neurocutaneous disorders can be classified into melanophakomatoses, vascular phakomatoses, and other phakomatoses. The most common phakomatoses (neurofibromatosis type I and II, tuberous sclerosis, von Hippel-Lindau disease, and Sturge-Weber-Dimitri syndrome) are not discussed in this article; however, we refer the readers to excellent reviews on these disorders.[8–10]

MELANOPHAKOMATOSES

Hypomelanosis of Ito (OMIM 300337)

Clinical Features

Hypomelanosis of Ito, also known as incontinentia pigmenti (IP) achromians, has an estimated prevalence of approximately 1/820,000 in the general population.[11] The disorder most commonly affects the skin, the central nervous system, and the musculoskeletal system. However, craniofacial, dental, cardiac, renal, and gonadal abnormalities may also be seen (Table 1).[12–17]

One of the hallmarks of this disorder is the distinctive pattern of the skin involvement, which is characterized by hypomacular zones with irregular borders, ''V'' or ''S'' shaped striations, swirls, patches, or whorls along the skin cell developmental lines of Blaschko (Fig. 1). These lesions involve mainly the trunk but can occur in the extremities, face, and scalp, usually sparing palms and soles.[12–14,16,18] This pattern of skin involvement is described as the ''negative image'' of that of IP. The term ''linear nevoid hypomelanosis'' has been proposed for cases with isolated skin involvement, whereas the term hypomelanosis of Ito would be reserved for cases with multiorgan involvement.[13]

Skin abnormalities are typically not associated with inflammatory signs and can be present at birth, which differs from the cutaneous changes seen in IP.[12,19] If not present at birth, approximately 75% of cutaneous abnormalities develop within the first year of life, and characteristically do not fade with age.[12,17] There is no correlation between severity of the disease and skin abnormalities.

Neurological symptoms are prevalent (affecting up to 80%–100% of the cases) but variable, and can include developmental delay, epilepsy, autism spectrum disorder, hyperkinesia, nystagmus, ataxia, sensorineural deafness, speech delay, and muscular dystonia. It may present with either macro- or microcephaly.[12–14,16,18]

Hypomelanosis of Ito has been associated with the development of several types of benign tumors including cystic teratoma of the mediastinum, complex mature sacrococcygeal teratoma, choroid plexus papilloma, dental hamartoma, and less commonly malignant tumors such as acute lymphoblastic leukemia, medulloblastoma, neuroblastoma, and primary meningeal rhabdomyosarcoma.[12]

Pathogenesis

Recent theories suggest that hypomelanosis of Ito is caused by a chromosomal mosaicism, which is not present in all cases. Autosomal dominant inheritance has been seen in some cases.[12,15,17]

Even though several genetic abnormalities have been reported, the 4 most commons defects are a short arm of X-chromosome (XP11), a short arm of chromosome 12, trisomy of chromosome 18, and triploidy.[17] Failure of X-inactivation may be the cause of sporadic cases.[17]

Imaging findings

Imaging findings are nonspecific. Brain magnetic resonance imaging (MRI) usually shows T2/FLAIR white matter abnormalities involving both the subcortical and periventricular white matter of the parietal lobes (Fig. 2A and B).[12,13,20] Cystic lesions and prominent perivascular spaces within the white matter signal abnormalities may be present (Fig. 2C and D), and diffuse brain atrophy with cerebellar hypoplasia is another possible feature.[12]

Migration and cortical organization abnormalities such as polymicrogyria, heterotopic gray matter, cortical dysplasia, and hemimegalencephaly (Fig. 3A, B, and C) have been described. Vascular anomalies including arteriovenous malformations (AVMs) and moyamoya vasculopathy have been described in association with hypomelanosis of Ito.[12,13] Neurological impairment is correlated with extent of CNS abnormalities.

TABLE 1. Clinical Features and Neuroimaging Findings in Melanophakomatoses

Melanophakomatoses	Clinical Features	Neuroimaging Findings
Hypomelanosis of Ito	Hypomacular lesions along the lines of Blaschko.	White matter changes associated with cystic lesions/proeminent perivascular spaces, predominant in the parietal lobes. Cortical migration abnormalities
Incontinentia pigmenti	Hyperpigmented lesions with inflammatory changes, along the lines of Blaschko.	Acute injury in the periventricular and subcortical white matter overlapping with areas of microhemorrhage. Sequelae of previous ischemic or hemorrhagic lesions on the cerebral hemispheres. Cortical migration abnormalities.
Neurocutaneous melanosis	Giant congenital melanocytic nevus.	Melanin deposition in the brainstem, cerebellum, amygdala, and along the leptomeninges.
Nevus of Ota	Bluish/brownish oculocutaneous lesions.	Intracranial melanoma with variable hemorrhagic component.
Waadenburg syndrome	Abnormal pigmentation of the skin and eyes, associated with dystopia canthorum and sensorineural hearing loss.	Dysplasia of the inner ear.
McCune-Albright syndrome	Café au lait skin changes associated with precocious puberty.	Fibrous dysplasia, commonly involving the craniofacial bones.

FIGURE 1. 10-Year-old boy with hypomelanosis of Ito presenting with cutaneous hypopigmentation changes along the lines of Blaschko on the left hemithorax, extending to the ipsilateral shoulder and arm.

Incontinentia Pigmenti (OMIM 308300)

Clinical Features

IP, also known as Bloch-Sulzberger syndrome, is an X-linked dominant disorder associated with a skewed X-chromosome inactivation in blood cells that is usually lethal in men,[21–25] with an estimated incidence of approximately 0.2 in 100,000 births.[26]

Most affected females will develop multiorgan abnormalities with a broad spectrum of involvement of the skin, hair, nails (eg, subungual benign tumors), teeth, eyes, and the CNS.[21–23,26–28] Affected patients also present with innate immunodeficiency, which leads to recurrent infections.[29]

Skin changes along the lines of Blaschko are present in virtually all affected patients,[28] and classically occurs in 4 stages: perinatal inflammatory vesicles, verrucous patches, hyperpigmentation (Fig. 4), and hypopigmented atrophy.[22,23,27,30] These stages are considered as major criteria for the diagnosis of IP.[23,27]

CNS abnormalities are reported in up to 30% of the cases and correlate with clinical symptoms, prognosis, and outcome.[27] Neurological symptoms occur early in life and are the major cause of morbidity in IP. Affected individuals usually present with developmental delay, seizures, and cerebral palsy.[22,23,28] The majority of patients have normal vision; however, vision abnormalities are linked to worse prognosis, and include retinal detachment, epitheliopathy, optic atrophy, microphthalmia, and blood vessel tortuosity.[22,23,30,31]

Pathogenesis

IP is believed to be caused by the IKBKG (inhibitor of kappa light polypeptide gene enhancer in B-cells, kinase gamma)/*NEMO* (NF-kappa-B essential modulator) gene. It is located in the Xq28 region, and encodes for a regulatory subunit of NF-kB signaling, involved in many regulatory functions such as immune/inflammatory responses, cell-growth, and apoptosis. IP is mostly a sporadic syndrome, and most of *IKBKG* mutations occur de novo.[21–23,28,32,33] Mutations that result in the loss of functions of the *IKBKG*/*NEMO* gene are lethal in men. Rarely, the mutation leads to mosaicism and is therefore not lethal, instead, these patients develop a disease similar to IP.[24,28] As the NEMO/inhibitor of nuclear factor kappa-B kinase gamma protein is enrolled in signaling pathways of several genes, its mutation can produce different phenotypes and outcomes, which can help explain the broad clinical spectrum of IP.[28,34,35]

Imaging Findings

The most common imaging features are brain infarction, lesions with atrophy involving the corpus callosum, and T2/FLAIR white matter signal hyperintensity,[22,23,27,31,36] which can occasionally be reversible.[37] Hemorrhagic and ischemic lesions have been widely reported (Figs. 5 and 6), especially in neonates. Although some studies have reported ischemic changes involving distinct vascular territories, in most cases lesions affect the microvasculature.[22,23,31,32,35]

Diffusion-weighted imaging may add specificity to the diagnosis in the presence of acute injury depicted as patchy, punctate, and confluent areas of restricted diffusion in the periventricular and subcortical white matter, basal ganglia, thalami, corpus callosum, and cerebellum.[22,36] Hypointense foci on susceptibility-weighted imaging (SWI), indicating microhemorrhages, may overlap with areas of acute injury on diffusion-weighted imaging (Fig. 7A–D).[22,36]

Other imaging findings include microcephaly, sequelae of injury such as focal cerebral atrophy and porencephaly, and developmental cortical abnormalities (Fig. 8A and B) including hemimegalencephaly. Vascular malformations may also be seen.[23]

Neurocutaneous Melanosis (OMIM 249400)

Clinical Features

Neurocutaneous melanosis (NC) is a rare disorder that presents with congenital pigmented nevi and CNS involvement which can be characterized by leptomeningeal or parenchymal melanin deposition, but classically without malignancy in the skin or nonmeningeal organs. Intracranial melanoma rarely occurs. Its prevalence is estimated approximately 1/50,000 to 1/200,000 births, with close to 30% to 50% of patients presenting with clinical symptoms.[38]

Children are most commonly diagnosed with NC when large or multiple congenital nevi (Fig. 9A) exist in association with meningeal melanosis or melanoma.[39] The risk of children with a giant melanocytic nevus to develop NC is unknown,[40] but studies have estimated it in approximately 7%. Patients with NC are at higher risk of developing melanoma, but malignant transformation is uncommon.[41]

Although asymptomatic disease is possible, symptoms usually manifest within the first 2 years of life. Neurological symptoms vary according to the location and extension of the brain lesion, and it tends to occur early in life. The most common clinical symptoms are seizures, cranial nerve palsy, myelopathy, radiculopathy, and hydrocephalus.[38] These symptoms are related to poor prognosis due to the higher association with the most severe spectrum of the disease: leptomeningeal melanosis.[40]

Pathogenesis

The pathogenesis of giant cutaneous nevus and NC is believed to be secondary to dysplasia of the neuroectodermal melanocytic precursor cells.[38]

Recent developments in genetics have included NC on the spectrum of the RASopathies. In a mouse model, embryonic somatic mutations in *NRAS* gene (chromosome 1p13) contribute to the

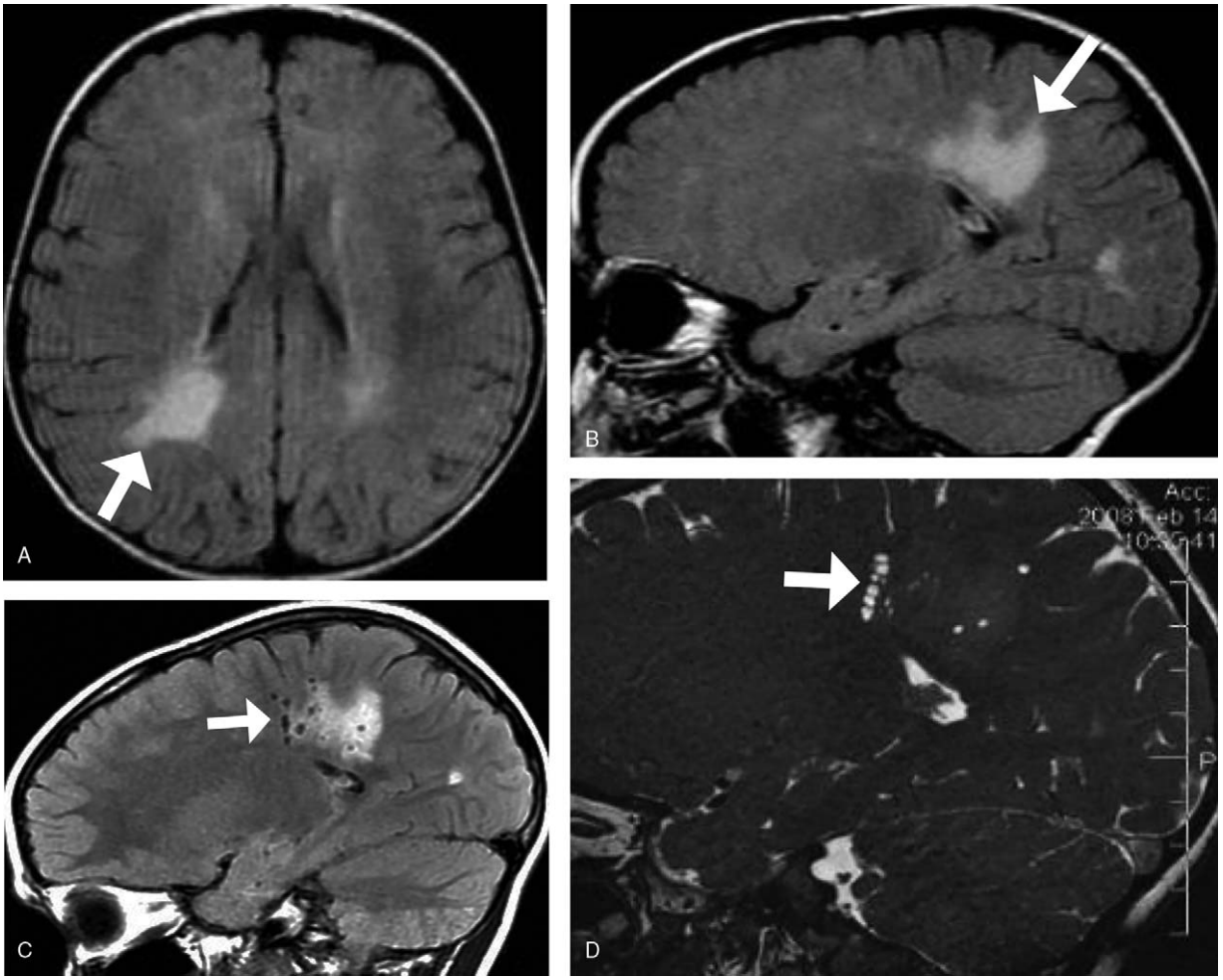

FIGURE 2. 1-Year-old infant with hypomelanosis of Ito. Axial (A) and sagittal (B) T2-FLAIR images show signal hyperintensity of the periventricular white matter, more prominent in the right parietal lobe (white arrows). Sagittal T2-FLAIR (C) and sagittal FIESTA (D) images after 2-year follow-up show prominent perivascular spaces within the periventricular and subcortical white matter of the right parietal lobe (white arrows).

pathogenesis of NC by activation of the NRAS GTPase, which is involved on intracellular signal flow and melanocytic cell lineage proliferation. Most probably the mutation occurs during the development of the neural crest or neuroectoderm.[40–47] The clinical outcome may vary according to additional chromosome abnormalities.[43]

Although rarer, BRAF mutations have also been described,[40,42,47–49] creating the prospect of new potential treatments with targeted molecular therapies such as BRAF inhibitors for patients with metastatic melanoma.[48,50]

Imaging findings

The cutaneous lesions are the hallmark of the diagnosis of NC; however, MRI plays a critical role in demonstrating CNS melanin deposition. MRI should be performed in all patients with giant melanocytic nevi, preferably within the first 6 months of life.[38,40,51–55]

Computed tomography (CT) can occasionally demonstrate melanocytic foci as hyperdense areas, but MRI is the method of choice. Melanin is better seen on nonenhanced T1-weighted images as parenchymal nodular or leptomeningeal linear T1 hyperintense lesions. NC lesions have a predilection for the cerebellum, brainstem, meninges, and temporal lobes, especially the amygdala (Fig. 9B).[38,51,54–56] In more severe cases MRI can show leptomeningeal thickening with contrast enhancement (Fig. 10A and B).

Isolated parenchymal deposition is associated with a better prognosis and is seen in less symptomatic patients.[40] Detection of melanotic deposition in the brain changes with time, as they tend to become less conspicuous with the progressing myelination.[40]

Affected patients are at a higher risk of developing melanoma. Malignant transformation to leptomeningeal melanoma occurs in approximately 40% to 65% of symptomatic cases.[38,56] Malignant transformation can be suspected by imaging by the presence of nodular/thick plaque-like contrast enhancement, adjacent parenchymal edema, lesion growth, and by the presence of necrosis and hemorrhage within the lesions.[38]

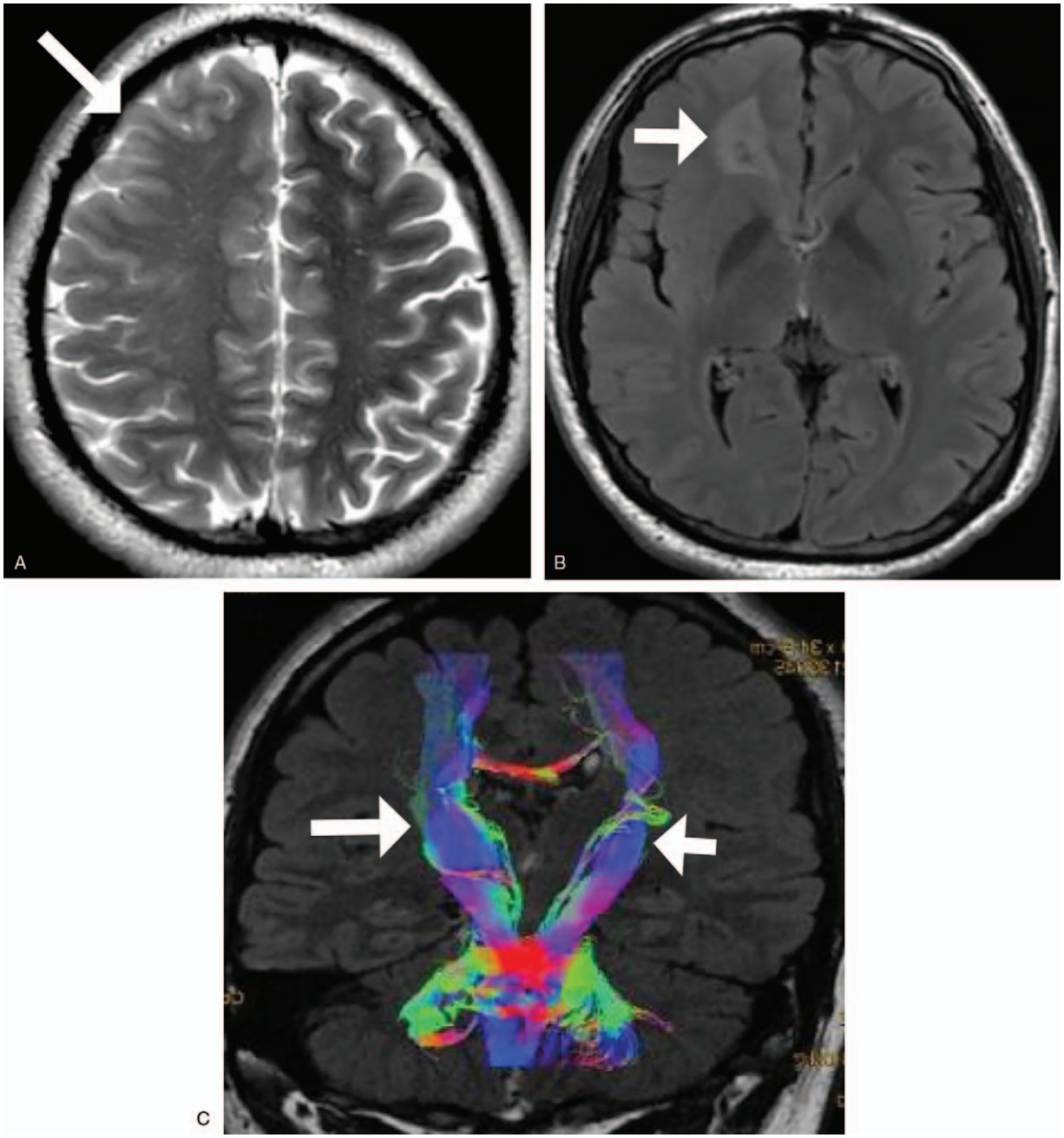

FIGURE 3. 27-Year-old man with hypomelanosis of Ito. Axial T2-weighted image (A) shows hemimegalencephaly of the right cerebral hemisphere (white arrow). Axial T2-FLAIR image (B) shows white matter signal abnormalities in the right frontal lobe (white arrow). Coronal T2-FLAIR with superimposed tractography (C) shows asymmetry of the corticalspinal tracts, the right (long white arrow) wider than the left (short white arrow).

Cerebellar hypoplasia may be seen.[55] In addition, approximately 10% of the affected patients present with a Dandy-Walker malformation. Both disorders probably relate to a disturbance in the formation of the cerebellar cortex and abnormal cerebrospinal fluid dynamics secondary to parenchymal and leptomeningeal melanin deposition.[38,57]

Nevus of Ota (ORPHA 263425)

Clinical Features

NO, also known as oculodermal melanocytosis, is a benign congenital melanocytic pigmentary disorder characterized by a blue hyperpigmented dermal lesion that affects the trigeminal dermatome,

FIGURE 4. 9-Year-old girl with incontinentia pigmenti presenting with hyperpigmented lesions in the right hemithorax and neck, with extension to the ipsilateral shoulder and arm, along the lines of Blaschko.

most commonly the V1 and V2 branches. It has a 5:1 female predilection and a unilateral pattern in 90% of the cases. In approximately 60% of the cases, the lesion is present at birth, and the other 40% will appear within the first decade of life.[7,58]

The lesion must be differentiated from the Mongolian spot, which is present at birth in up to 90% of the cases and it usually disappears in puberty, as opposed to NO, which tends to become more visible with progressing age. The classic description of the skin pigmentation includes a deeper bluish color with superficial brownish areas, but this pattern is more commonly seen in the eyes (Fig. 11A).[7,59]

Ocular involvement occurs in up to 50% of the cases. Affected patients are at a higher risk of developing uveal melanoma than the general population, and it can very rarely develop malignant transformation into cutaneous meningeal and dural melanoma.[59–62] NO has also been associated with other disorders such as Takayasu arteritis, Klippel-Trenaunay-Weber syndrome, AVMs, neurofibromatosis type I, and spinocerebellar degeneration among others.[7]

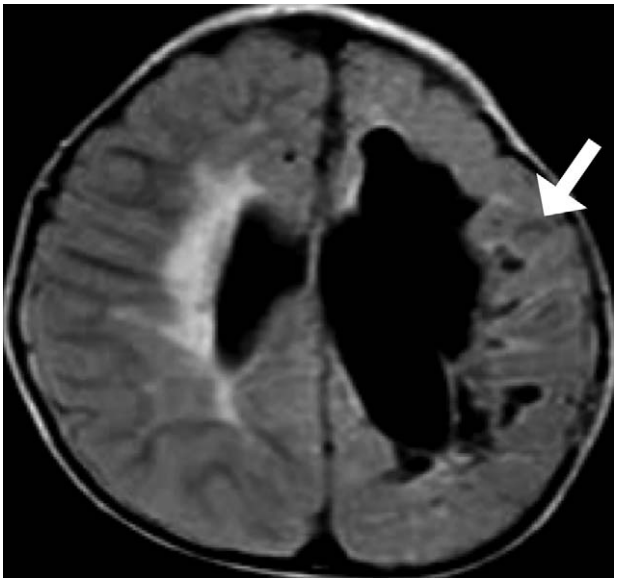

FIGURE 5. 10-Year-old girl with incontinentia pigmenti. Axial T2-FLAIR image shows atrophy and gliosis of the periventricular white matter bilaterally, consistent with sequelae of parenchymal injury, as well as compensatory enlargement of the left lateral ventricle (white arrow).

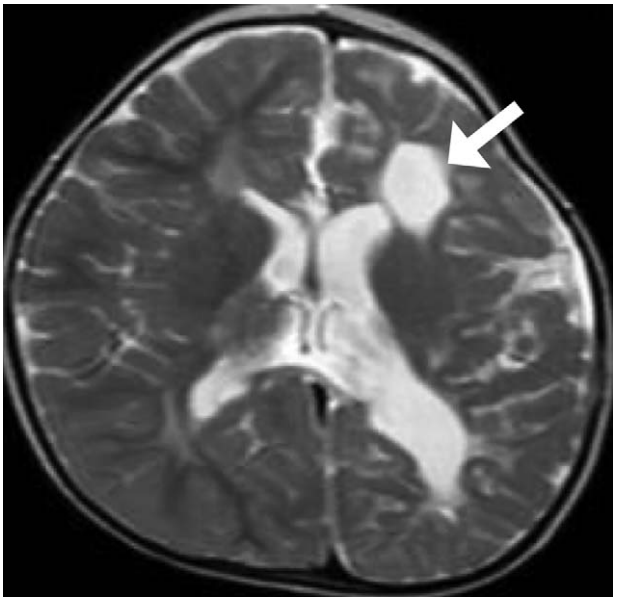

FIGURE 6. Incontinentia pigmenti. Axial T2-weighted image shows sequelae of parenchymal injury associated with atrophy of the left hemisphere, with compensatory enlargement of the left lateral ventricle, and areas of cystic transformation of the periventricular white matter (white arrow).

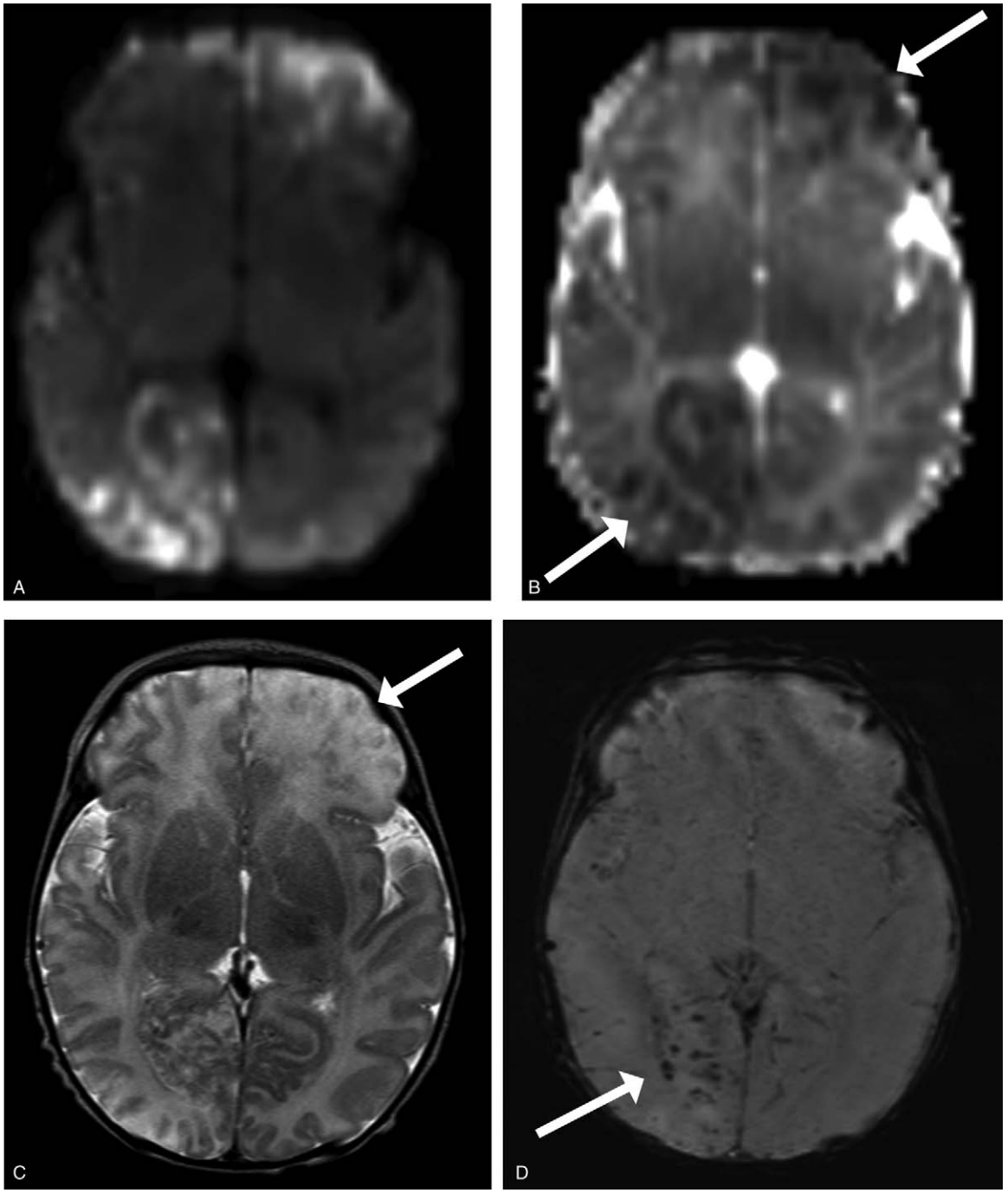

FIGURE 7. 6-Year-old girl with incontinentia pigmenti. Axial diffusion-weighted imaging (DWI) (A) and ADC map (B) show multifocal parenchymal diffusion restriction involving predominantly the cortex of the left frontal and right occipital lobes, consistent with acute cytotoxic injury. Axial T2-weighted image (C) shows cortical edema in the left anterior frontal lobe. Axial SWI image (D) shows microhemorrhagic foci within the right occipital lobe.

Pathogenesis

It is believed that NO develops due to incomplete migration of melanocytes of the neural crest to the epidermis during embryogenesis.[7,58] Two main causative mutations were identified: *GNAQ* (a mutation also present in uveal melanomas) and *MMP10*. Interestingly, NO often overlaps histologically with a blue nevus, which also harbors the *GNAQ* mutation in up to 80%.[59,61] It is suggested that in cases in which NO harbors *GNAQ* and *MMP10* mutations it may evolve to melanoma by acquiring *BAP1*, *COL4A4*, *PLD3*, and *FN3K* mutations.[61] These mutations may serve as a basis to develop targeted molecular therapies.[61]

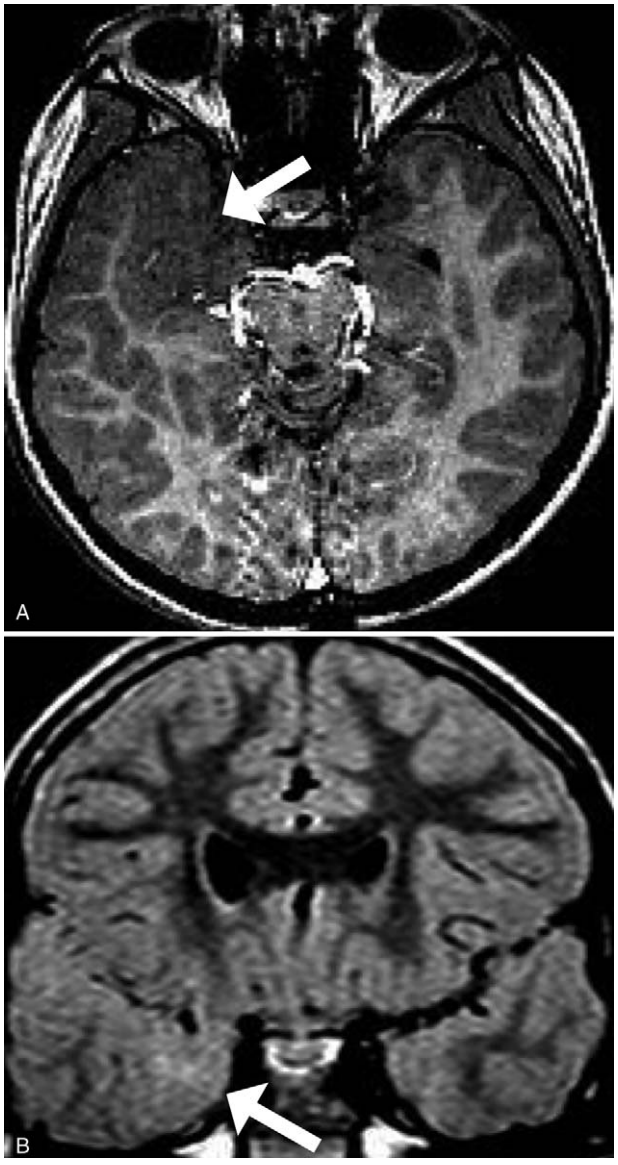

FIGURE 8. Young adult female with incontinentia pigmenti. Axial contrast-enhanced T1-weighted (A) and coronal T2-FLAIR (B) images show cortical dysplasia in the right temporal lobe (white arrows) characterized by thickening of the cortex, blurring of the grey-white matter junction, and FLAIR signal hyperintensity of the subcortical white matter.

Imaging Findings

Patients with NO may present with intracranial melanoma, which can appear as hemorrhagic lesions (Fig. 11B and C) and tends to occur in the cerebral hemispheres, optic chiasm, optic tract, and pineal gland.[7]

Meningeal primary melanomatosis may also be seen, characterized by T1 hyperintensity along the subarachnoid spaces. Another less common lesion is meningeal melanocytoma, which can have a variable presentation on imaging depending on the degree of myelination. On CT they usually appear as hyperdense lesions, with variable contrast enhancement. On MRI they correlate with melanin signal.[7,63,64]

MRI has a critical role in surveillance for possible malignant transformation. Malignant transformation is suspected when there are growing masses, change in the signal intensity pattern and infiltration of previously uninvolved structures. Positron emission tomography (PET) may be useful in detecting malignant transformation of the NO.[60]

Another imaging findings include ocular melanoma and facial bone abnormalities typically with a hypertrophy pattern, with thickening of the orbital wall and the paranasal sinuses.[60,65]

Waardenburg Syndrome (OMIM 277580)

Clinical Features

Waardenburg syndrome (WS) is a rare inherited disorder, with an estimated prevalence of 1/40,000 births, characterized by abnormal pigmentation of the skin, hair, and eyes, dystopia canthorum (lateral displacement of the inner canthi of the eyes), and various degrees of sensorineural hearing loss.[66–70] It is responsible for approximately 1% to 3% of all cases of congenital deafness.[66] Although pigmentary changes and congenital deafness are its most characteristic features, WS includes a more variable spectrum of abnormalities, which are separated into 4 distinct clinical subtypes.[67,68,70,71] Facial dysmorphism is mainly present in WS types 1 and 3; however, musculoskeletal abnormalities are usually absent in WS type 1. WS type 2 is characterized by all the classical clinical features seen in WS, except for dystopia canthorum. Association with Hirschsprung disease is characteristic of WS type 4.[68,69] Neural tubes defects such as spina bifida are more common in WS type 1 and 3 than in the general population.[68] Myelomeningocele, when present, is associated with a dramatic reduction in quality of life.[68]

Pathogenesis

Six related genes have been described: *PAX3*, *MITF*, *EDN3*, *EDNRB*, *SNAI2*, and *SOX*.[67,71] There is a positive correlation between clinical symptoms and genetic abnormalities.[69] *SOX10* is the most common mutation associated with WS and is responsible for 15% of WS type 2 and 40% of WS type 4. *SOX10* is involved in the development of neural crest derivatives and in the development of the glia, oligodendrocytes and also Schwann cells.[67] Patients that harbor SOX10 mutation have a poor prognosis due to severe neurological symptoms, mainly caused by myelination abnormalities of the central and peripheral nervous system.[66] *PAX3* is mostly expressed in the neural crest and is the primary cause of WS types 1 and 3.[68,69] Severe neural tube defects are usually related to *PAX3* mutations and are most commonly seen in WS type 3. WS type 2 shows mutations in the *MITF* (microphthalmia-associated transcription factor) and SRY (sex determining region)-box 10 (*SOX10*) in approximately 15% each. Mutations in the *EDNRB* (endothelin receptor type B), *EDN3* (endothelin 3), and in the *SNAI2* (snail family zinc finger 2) are seen in fewer than 5% of the cases.[69] Mutations in the *MITF* gene are correlated with several ocular abnormalities.[70]

Imaging Findings

Neural tubes defects are relatively common, particularly myelomeningocele. Several abnormalities of the inner ear are also described. The most common involve the semicircular canals—agenesis of the posterior and superior semicircular canal is most frequently seen. Other findings may include enlargement of the vestibular aqueduct, obliteration of the oval window, or narrowing of the internal auditory canal.[66,72]

McCune-Albright Syndrome (OMIM 174800)

Clinical Features

McCune-Albright syndrome (MAS) is a rare congenital disorder with an estimated prevalence between 1/100,000 and

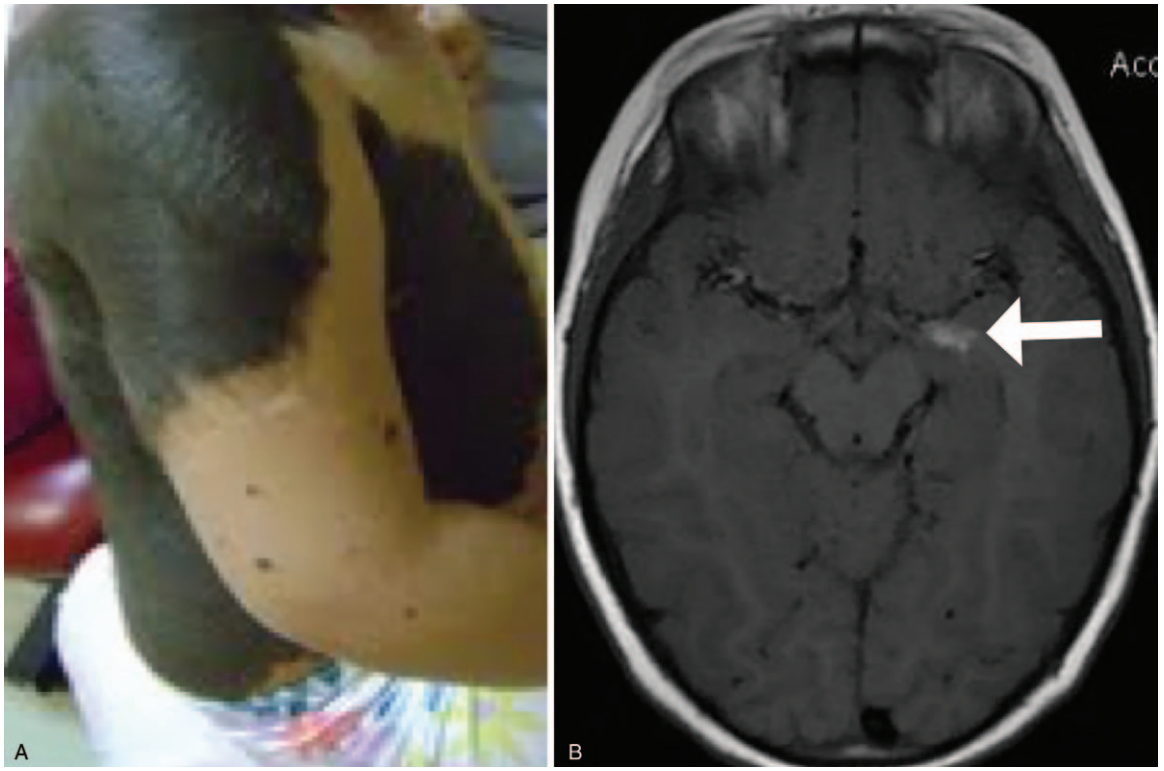

FIGURE 9. Male child with neurocutaneous melanosis presenting with a giant melanocytic nevus involving the dorsal region, posterior cervical region, right arm, and anterior abdominal wall (A). Axial unenhanced T1-weighted image (B) shows a hyperintense nodular/linear lesion in the left amygdala, consistent with melanin deposition (white arrow).

1/1,000,000,[73] characterized by a clinical triad of fibrous dysplasia (FD; monostotic or polyostotic), skin abnormalities (classical café au lait skin pigmentation) and precocious puberty.[74–77] When the classic clinical triad is incomplete, establishing the correct diagnosis may be challenging.

Affected individuals may also develop several endocrinopathies and gastrointestinal abnormalities.[78] Skeletal abnormalities usually present with limb/rip pain, progressive scoliosis, or pathologic fractures.[73] Usually, the typical skin changes of MAS first appear shortly after birth, and bear no correlation with disease severity.[79]

Patients with MAS carry a higher risk of developing testicular cancer secondary to high serum levels of testosterone.[79]

Pathogenesis

MAS is caused by a postzygotic somatic activating mutation at the *GNAS* gene (located in chromosome 20q13), which is responsible for encoding the G-protein alpha subunit (Gsα). Activation of the Gsα leads to activation of the cAMP pathway, which is responsible for endocrine abnormalities and overproduction of melanocytes, resulting in the typical skin changes seen in the syndrome.[74–76,79–82] Affected individuals usually present with mosaic genetic patterns.[79] The higher the mosaicism, the more severe the disease phenotype.[76] The *GNAS* mutation is confirmed by biopsy of affected bone.[77]

Imaging Findings

The most common imaging finding is FD, which can be monostotic or polyostotic, commonly involving the craniofacial bones (25%–30%).[74,75] Clinical symptoms vary according to the region involved. The pattern of FD varies from predominantly lytic lesions to the classic ground glass appearance seen in the majority of cases.[75,79]

CT is the criterion standard for the characterization of osseous abnormalities; however, MRI better depicts soft tissue components and the effects of bone changes on adjacent structures such as the optic nerves.[75,83] Malignant transformation of FD is extremely rare; however, there are reports of sarcomatous transformation within FD lesions.[79]

VASCULAR PHAKOMATOSES

Hereditary Hemorrhagic Telangiectasia (OMIM 187300)

Clinical Features

Hereditary hemorrhagic telangiectasia (HHT), also known as Rendu-Osler-Weber disease, is a rare and highly penetrant autosomal dominant vascular neurocutaneous disorder with a prevalence of 1/10,000 births. The hallmark of the disorder is the presence of AVMs that may involve many organs and tissues such as CNS, lungs, and gastrointestinal tract (Table 2).[84,85]

Diagnostic criteria for HHT are called Curaçao criteria, in which HTT is ''definitive'' if at least 3 out of the 4 classical features are present: epistaxis, telangiectasia, visceral lesions, and positive family history (first-degree relative). HTT is ''suspected'' if the patient has 2 of these features, and ''unlikely'' if only 1 feature is present.[85–88] If a positive family history is present, active search for other cases, especially among children, is crucial.[84,89,90]

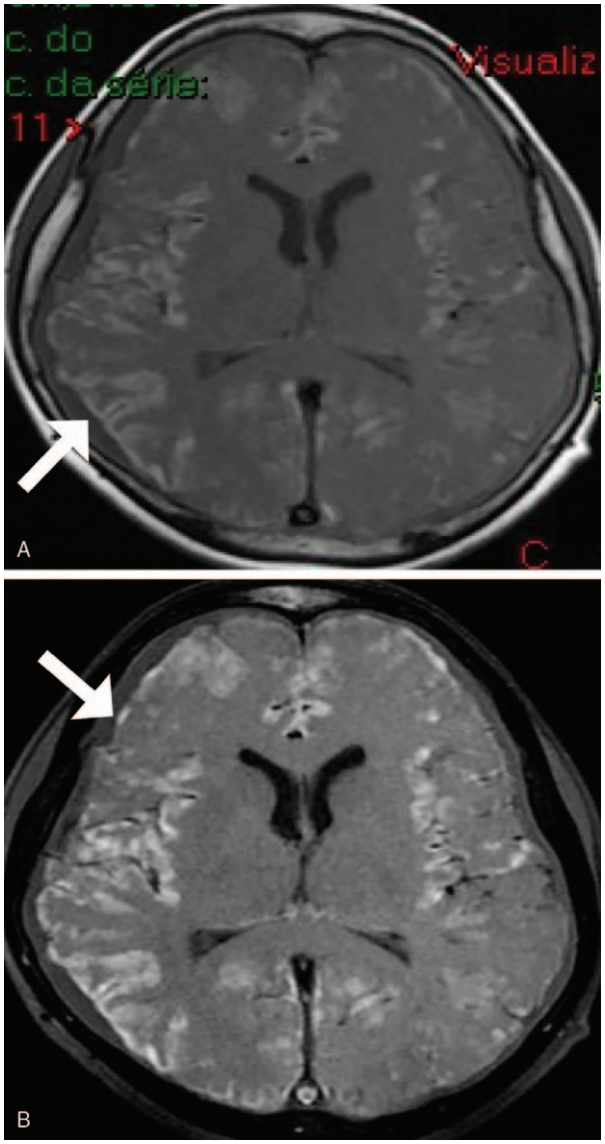

FIGURE 10. 12-Year-old man with neurocutaneous melanosis. Axial unenhanced (A) and contrast-enhanced (B) T1-weighted images show signal hyperintensity, slight contrast enhancement, and thickening of the leptomeninges of the right greater than left cerebral hemispheres (white arrows).

Affected individuals most commonly develop anemia secondary to chronic bleeding, usually due to recurrent epistaxis or gastrointestinal hemorrhage. However, a significant number of patients present with acute severe pulmonary hemorrhage secondary to pulmonary AVMs manifesting as massive hemoptysis or hemothorax.[85,86]

Others possible symptoms and complications of AVMs in HHT are migraine, seizures, ischemic or hemorrhagic stroke, cardiac failure, and brain abscess.[86–88,91] The risk of a rupture of cerebral AVMs in HHT is lower than in children with sporadic AVMs.[89,91–93]

Mucocutaneous vascular lesions of HHT may be visible on physical examination as small, sometimes pulsatile, linear reddish lesions (Fig. 12A).[84]

Pathogenesis

Current evidence suggests that HHT is caused by an enhanced response to angiogenic stimulus in ALK1 and reduced BMP signaling, a pathway crucial for development and maintenance of the vascular and lymphatic circulation.[94,95]

Four genes have been associated with HHT development: *ENG*, *ACVRL1*, *SMAD4*, and *GDF2/BMP9*. The vast majority of the cases (approximately 96%) are caused by *ENG* and *ACVRL1*, which are located in the chromosome 9q34 and chromosome 12q13, respectively.[85,86,88,92,94,96–98] All of these genes are involved in the transforming growth factor beta signaling pathway, which plays an essential role in maintaining vascular integrity. A genotype-phenotype correlation exists: patients with mutations in the *ENG* gene are more likely to develop multiple lesions including pulmonary AVMs, and therefore a more severe pattern of disease, whereas patients with the *ACVRL1* mutation are more likely to develop hepatic and gastrointestinal AVMs.[88]

Imaging Findings

Numerous vascular malformations are associated with HHT, including cavernous malformations, dural AV-fistulas, aneurysms, and AVMs.[91] Typically, the cerebral AVMs have a small nidus (''micro AVMs'') and are located superficially and in the supratentorial compartment (Fig. 12 B, C, and D), which usually correlates with a low Spetzler-Martin grade.[92,93,99] Although cerebral AVMs occur both in children and adults, pulmonary AVMs are more frequent in adults (Fig. 12E).[91,92,99]

Ataxia Telangiectasia (OMIM 208900)

Clinical Features

Ataxia telangiectasia (AT) is a rare autosomal recessive progressive neurodegenerative disorder with a prevalence of 1 to 40,000 to 100,000 births.[100–103] AT is the most common cause of cerebellar ataxia in children younger than 5 years of age and the second most common pediatric neurodegenerative disorder involving the cerebellum.[102,104] Children of consanguineous marriage carry a higher risk for AT.[102,105–108] AT is classically associated with high and progressive serum levels of alpha-fetoprotein, which may serve as a diagnostic clue.[102]

Ocular abnormalities and visual impairment are main concerns in AT given its high prevalence, and a significant cause of morbidity.[100] Oculocutaneous telangiectasias have been classically related to AT (Fig. 13A) but may not be present in early stages of the disease, and do not correlate with vision loss.[100,103,109,110]

Affected children also present with signs of immunodeficiency (sometimes one of the first symptoms are recurrent sinopulmonary infections). In addition, these children can develop insulin resistance, gonadal failure, growth retardation, and a higher risk for cancer development, mostly lymphoid malignancies.[100–103,111,112] Heterozygous carriers also have a higher cancer predisposition.[102,113]

Neurological symptoms appear in the early stages of the disease, most commonly within the first year of life, and consist of ataxia, oculomotor apraxia, and extrapyramidal symptoms.[100,101] Although these are the most common neurological symptoms, the spectrum is much broader. Affected patients may present with other movement disorders such as dystonia, choreoathetosis, tremors, myoclonus, as well as peripheral neuropathy and absence of deep reflexes.[102,103,110,111]

Pathogenesis

AT is caused by a mutation in the ATM gene located in chromosome 11q 22–23.[102,103,114] The ATM gene plays several

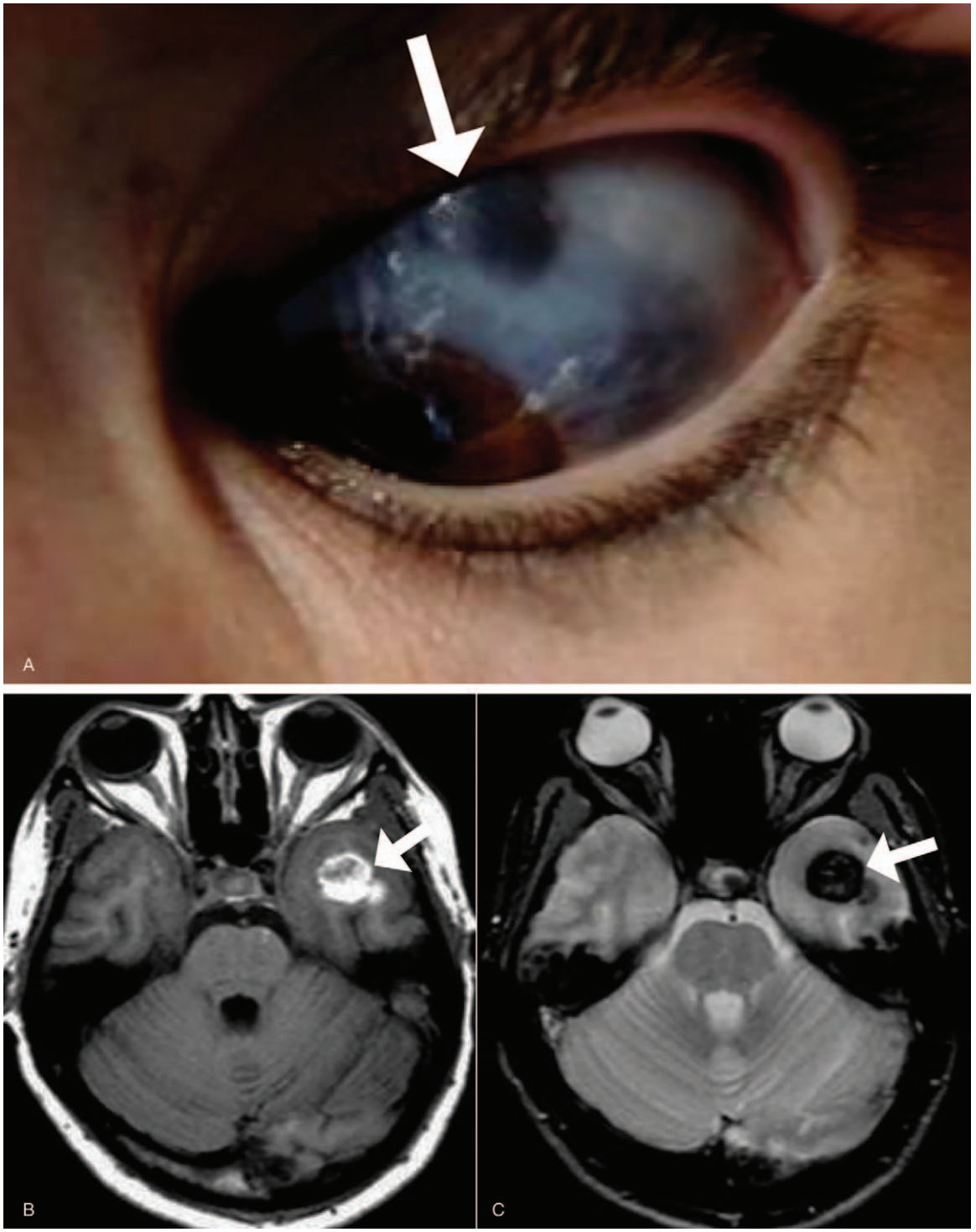

FIGURE 11. Nevus of Ota. Brownish and bluish areas on the sclera of the left eye (A). Axial unenhanced T1-weighted image (B) and axial T2* (GRE) (C) show a nodular lesion in the left temporal lobe, presenting with T1 signal hyperintensity and marked signal hypointensity on GRE, which may represent melanin deposition and/or blood products (white arrows).

TABLE 2. Clinical Features and Neuroimaging Findings in Vascular Phakomatoses

Vascular Phakomatoses	Clinical Features	Neuroimaging Findings
Hereditary hemorrhagic telangiectasia	Epistaxis, mucocutaneous telangiectasias, chronic anemia, and family history.	Vascular malformations, commonly AVMs with small nidus.
Ataxia-telangiectasia	Ataxia with high AFP serum levels.	"Pure" cerebellar atrophy.
Wyburn-Mason syndrome	Variable	High-flow AVMs involving the optic apparatus
Cobb syndrome	"Port-wine" stain, usually on the trunk. Can be asymptomatic.	Spinal AVMs involving the same metamere as the skin change. Vertebral hemangiomas with soft tissue and epidural component.
Klippel-Trenaunay-Weber syndrome	Varicose veins, cutaneous capillary malformation and bone and soft tissue overgrowth. Overlap with other cutaneous disorders.	Leptomeningeal angiomatosis, hemimegalencephaly, parenchymal calcifications.
PHACES syndrome	Facial hemangioma involving the trigeminal territories, cardiac defects, coarctation of the aorta, eye, and sternal abnormalities.	Posterior fossa malformation, neurovascular abnormalities, and ischemic stroke.
Blue rubber bleb syndrome	Multiorgan venous malformations and anemia due to chronic gastrointestinal bleeding.	Venous and capillary malformations.

AFP indicates alpha-fetoprotein.

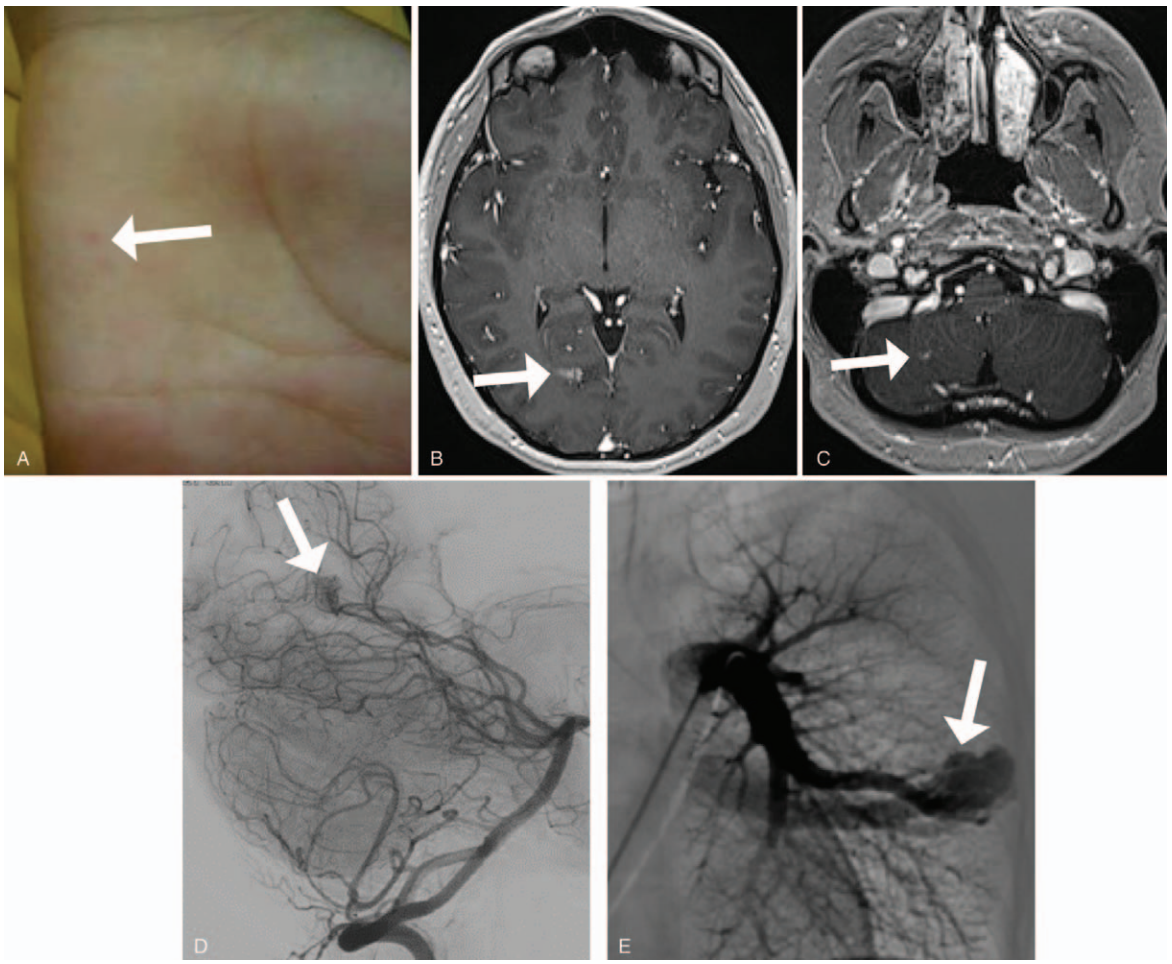

FIGURE 12. 26-Year-old woman with HHT. Cutaneous telangiectasia in the palm of the left hand (white arrow in A). Axial contrast-enhanced T1-weighted images (B and C) show ill-defined areas of enhancement in the right occipital lobe (white arrow on B) and in the right cerebellar hemisphere (white arrow on C), compatible with small arteriovenous malformations. Digital cerebral angiography (D) shows a small AVM in the right occipital lobe (white arrow), supplied by the calcarine artery. Digital pulmonary angiography (E) shows a high-flow pulmonary AVM in the left lung (white arrow).

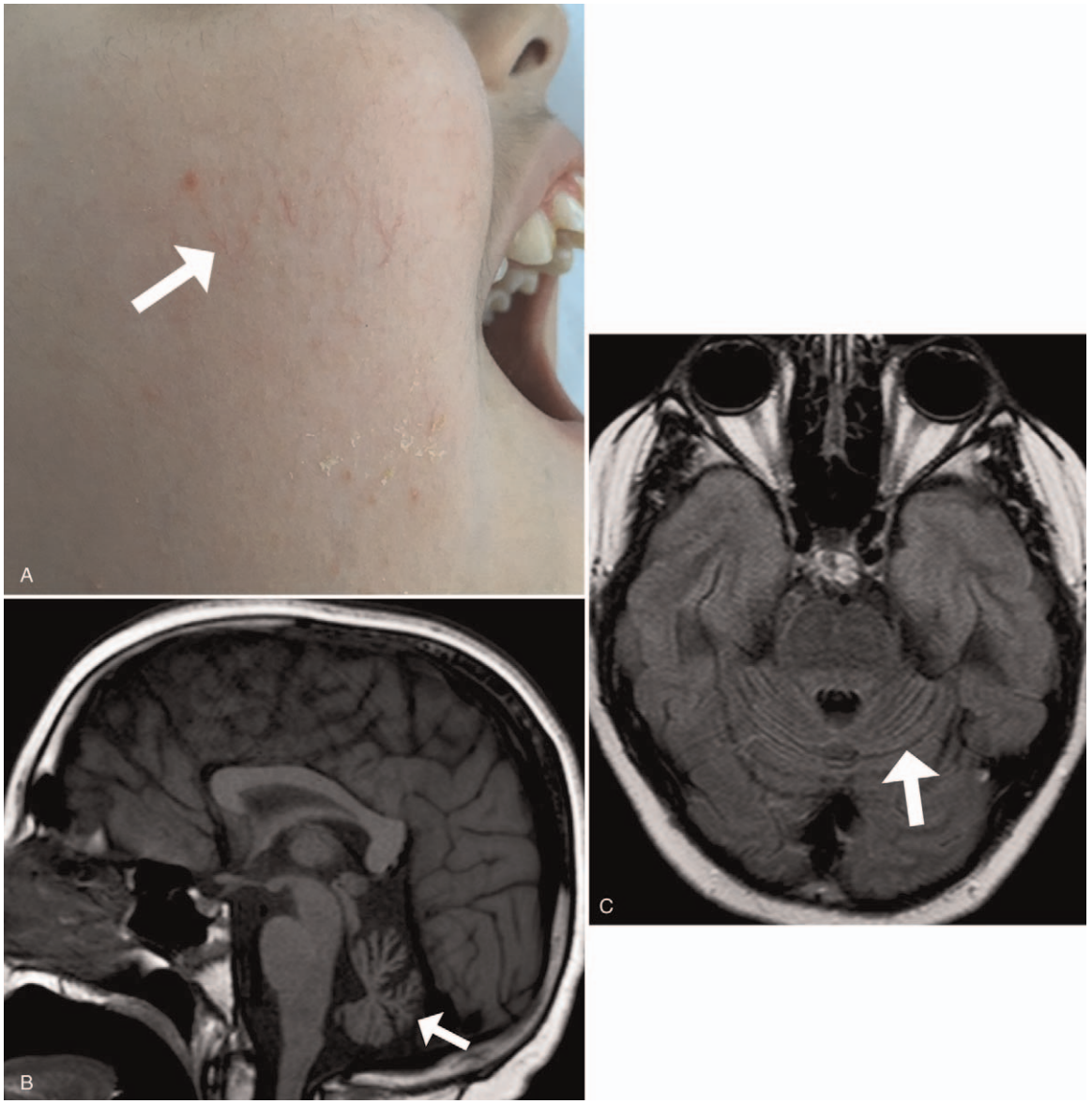

FIGURE 13. 11-Year-old boy with ataxia-telangiectasia. Cutaneous telangiectasia on the right cheek (white arrow on A). Sagittal unenhanced T1-weighted image (B) and axial T2-FLAIR images (C) show diffuse cerebellar atrophy (white arrow on B) without signal abnormalities in the cerebellar cortex (white arrow on C).

roles in different tissues, including protein activation, apoptosis, cell cycle checkpoint control, and DNA repair. Mutation in the ATM gene leads to increased oxidative stress and progressive DNA damage.[102,103,111] Knowledge regarding the many functions of the ATM gene explains many clinical features of AT, such as sensitivity to radiation and cancer predisposition.[102,111,115–117]

Imaging Findings

On MRI, patients with AT frequently present with early onset of progressive cerebellar atrophy, sometimes predominantly affecting the vermis without signal intensity abnormalities of the cerebellar cortex (Fig. 13B and C).[102,110,118] There is no established correlation between the degree of cerebellar atrophy and the severity of clinical symptoms.[100,118] Cerebral white matter changes have also been described, either T2 hyperintensity or hypointensity, probably attributed to demyelination or capillary telangiectasia, respectively.[118]

Wyburn-Mason Syndrome (ORPHA 53719)

Clinical Features

Wyburn-Mason syndrome (WMS), also known as Bonnet-Dechaume-Blanc syndrome, is a very rare neurocutaneous disorder with approximately 100 reported cases. It is recognized as a form of metameric vascular dysplasia.[119–122] No familial forms or risk factors have been described. WMS is characterized by the association of high-flow AVMs involving the brain and the optic apparatus with a variable subtle reddish-bluish cutaneous nevus that commonly affects the trigeminal territory.[119,122]

Affected patients usually become symptomatic during childhood, although the nevus can be present at birth. Symptoms vary according to the size and location of the AVMs, but the most common presentation is progressive vision loss.[119,121] AVMs in WMS occur at a much younger age than sporadic AVMs.[119,122] Although the classical features are seen in the majority of the cases, WMS is considered to be part of a broader spectrum which includes orbital AVMs that spare the retina, and bilateral ocular AVMs or multifocal brain lesions.[119,121]

Neurological symptoms are variable and nonspecific, with the affected individuals usually presenting with headache, focal deficit, and seizures. There is also a higher risk of severe and occasionally life-threatening epistaxis and gingival bleeding due to high-flow AVMs.[121,122]

Pathogenesis

WMS appears to be caused by an early insult in the primitive vascular mesoderm, which will later develop the neural tube and the optic cup.[122–124] This theory explains the metameric distribution of unilateral WMS; however, bilateral cases have also been reported; their pathogenesis remains to be fully elucidated.[122]

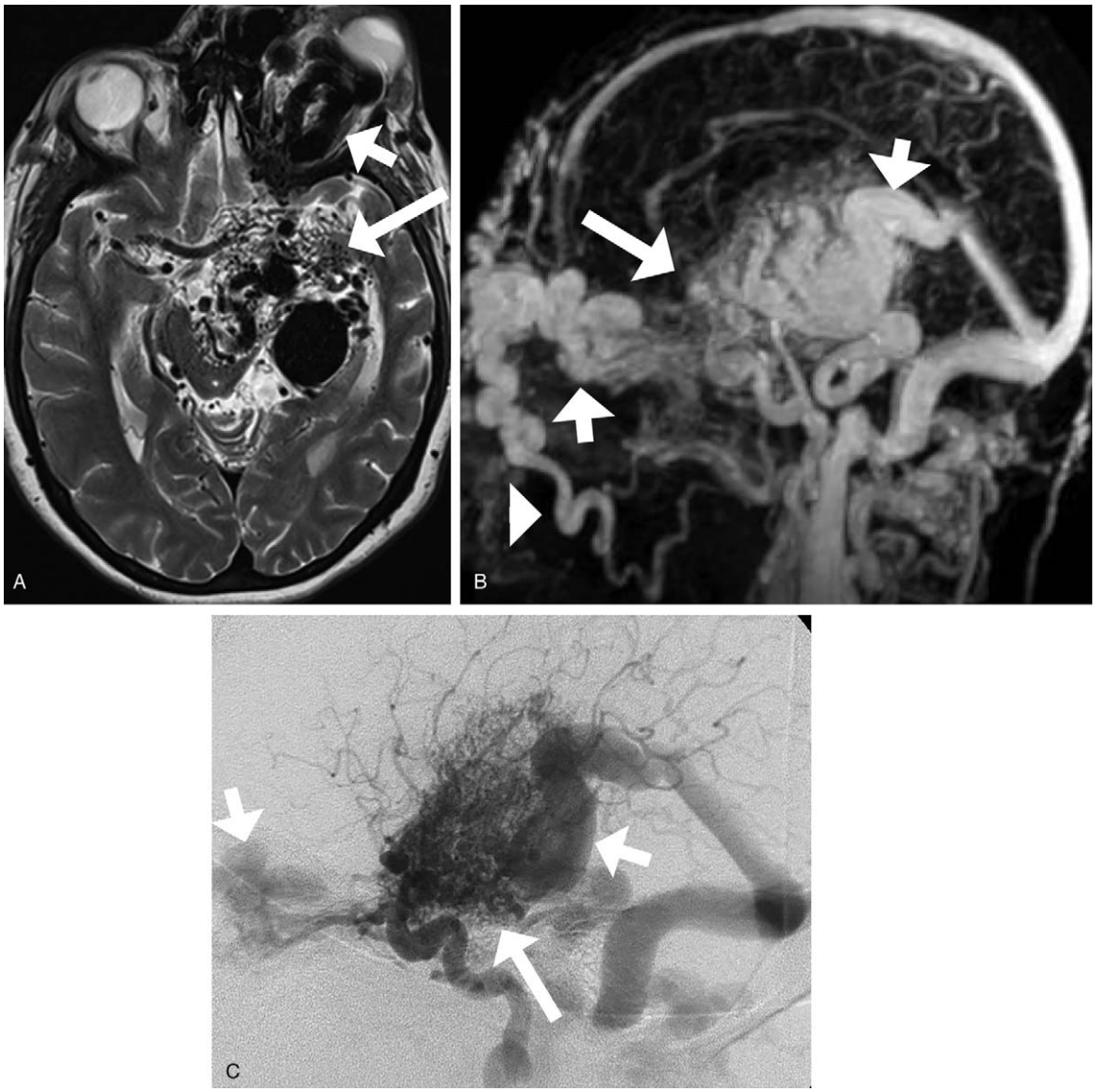

FIGURE 14. 28-Year-old woman with Wyburn-Mason syndrome. Axial T2-weighted (A) image shows a large high-flow AVM involving the left optic apparatus including the left orbit (short white arrow), left optic nerve, optic chiasm and also the temporal lobe (long white arrow). Sagittal magnetic resonance venography image (B) shows the high-flow AVM involving the left optic apparatus (long white arrow) with venous drainage to the superior ophthalmic vein and to the deep venous system (short white arrows). There is also retrograde opacification of the left facial vein (white arrowhead). Digital cerebral angiography (C) shows the high-flow AVM involving the left optic apparatus (long white arrow) with venous drainage to the superior ophthalmic vein and to the deep venous system (short white arrows). Courtesy of Dr. Marcos M. B. Negreiros, Botucatu, Brazil.

Imaging Findings

WMS is characterized by unilateral high-flow AVMs involving the optic apparatus and the brain, most commonly the optic nerve, optic chiasm, retina, cerebral hemispheres, thalamus, and basal ganglia. Lesion location can be highly variable (Fig. 14A, B, and C). The internal carotid artery is most commonly responsible for the arterial supply, whereas venous drainage via the vein of Galen or cavernous sinus is seen with deep lesions.

Cobb Syndrome (ORPHA 53721)

Clinical Features

Cobb syndrome (CS) is a rare sporadic disorder characterized by spinal AVMs associated with cutaneous ''port-wine'' stains involving the same metamere. It has an unknown prevalence, with approximately 100 reported cases.[125,126] CS is recognized as a spinal arteriovenous metameric syndrome, which is defined by the presence of separate vascular malformations involving the same metamere.[125,126]

Although classically described with ''port-wine'' stains in the skin (Fig. 15A), the cutaneous abnormalities have a broader spectrum including angiomas, keratomas, angiolipomas, and lymphangiomas, which do not involute with time.[125] Unlike many phakomatoses, CS can remain asymptomatic for a long period; patients may only seek medical attention for esthetical purposes or due to cutaneous bleeding after local trauma.[125] Affected patients can also present with neurological symptoms secondary to cerebral or spinal cord compression, congestive edema, ischemia, or hemorrhage. Presenting symptoms are focal deficit, paraplegia, headache, and neurogenic bladder.[125,126]

Pathogenesis

As with others cutaneous-vascular malformations with metameric distribution, CS is believed to be caused by an insult to the primitive vascular mesoderm before its migration.[92]

Imaging Findings

MRI is the exam of choice to depict spinal AVMs and to evaluate intramedullary signal changes.[125,127,128] CS may also present with multiple vertebral body venous malformations (formerly referred to as hemangiomas) associated with soft tissue component that may invade the spinal canal (Fig. 15B and C).[127]

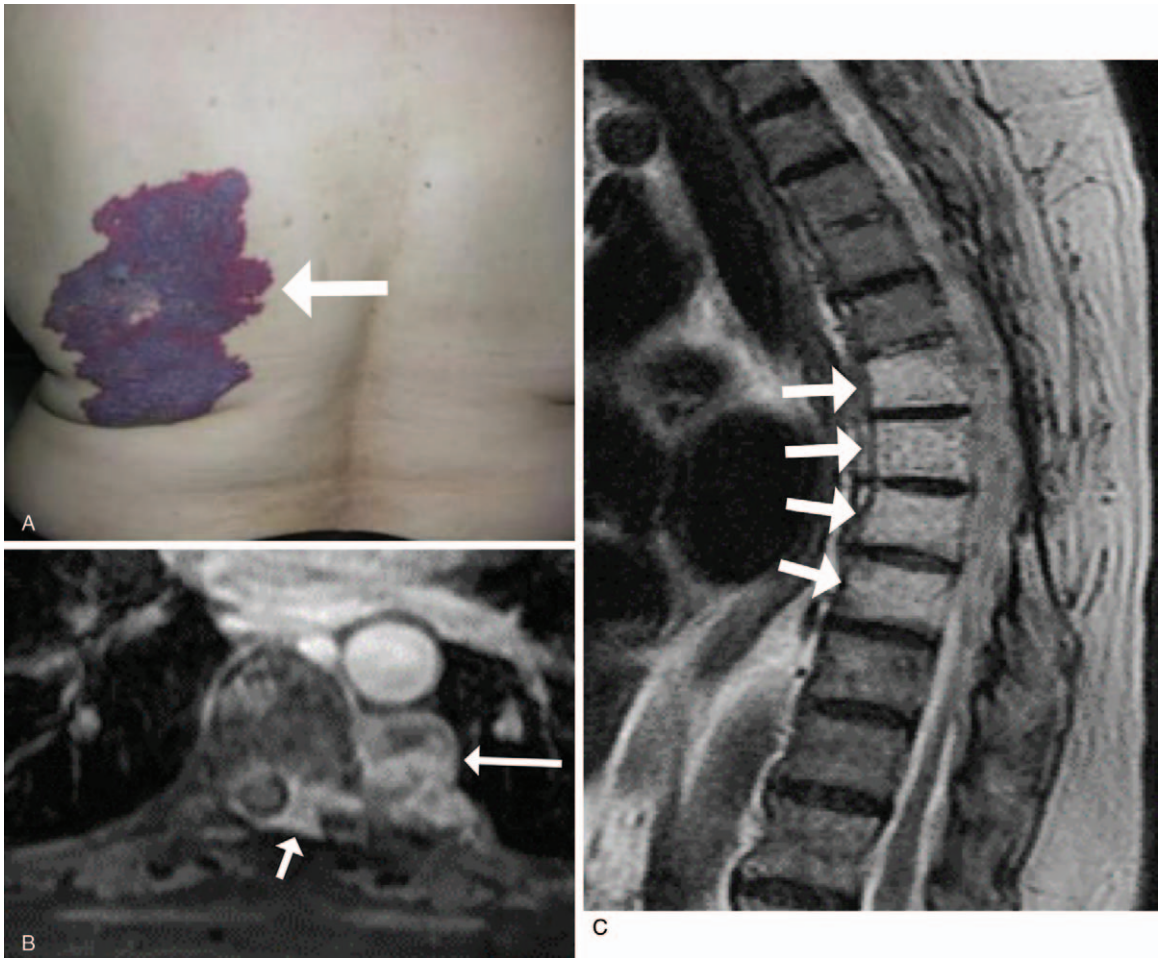

FIGURE 15. Male adult with Cobb syndrome. Cutaneous ''port-wine'' stain on the back (white arrow on A). Axial contrast-enhanced T1-weighted image (B) shows an enhancing left paraspinal thoracic venous malformation (long white arrow) with an adjacent epidural component (short white arrow). Sagittal T2-weighted image (C) shows multiple vertebral venous malformations ("hemangiomas'') involving contiguous thoracic vertebral bodies (white arrows). Courtesy of Dr. Marcelo Canuto, Brasília, Brazil.

Conventional angiography can add relevant information regarding the angioarchitecture of the AVMs, as well as for therapeutic planning.[125–127,129,130] The correct identification of AVM location is crucial because it may contraindicate lumbar puncture.[125]

Klippel-Trenaunay-Weber Syndrome (OMIM 149000)

Clinical Features

Klippel-Trenaunay-Weber syndrome (KTWS) is a rare and most commonly sporadic multiorgan disorder. It has been recently recognized as part of PROS (PIK3CA-related overgrowth spectrum), characterized by congenital cutaneous capillary malformations (''port-wine'' stain), venolymphatic malformations, and growth disturbances (mainly segmental hypertrophy).[131–135]

PROS include several overgrowth disorders previously considered separate entities, but currently known to be similar disorders with highly overlapping phenotypes, such as megalencephaly-capillary malformation and congenital lipomatous overgrowth, vascular malformation, and epidermal nevi syndromes.[132] Overlap between KTWS and Sturge-Weber syndrome has also been described in the literature (Fig. 16).[136,137]

The ''port-wine'' stains can appear on several different locations (Fig. 17A), and together with bone and soft tissue hypertrophy are present in more than 90% of the cases. Hypertrophy is usually unilateral and the lower limbs are mainly affected, although it can affect the upper extremities and less frequently the trunk.[131,132] Congenital varicosity is also very common (up to 75%), as are lymphedema, swelling, gastrointestinal bleeding, and digital abnormalities such as syndactyly and polydactyly.[131–133]

FIGURE 16. 8-Month-old male infant with an overlap of Klippel-Trenaunay-Weber and Sturge-Weber syndromes presenting with cutaneous lesions on the face and thorax (not shown). Axial unenhanced CT shows gyriform calcifications associated with atrophy of the right cerebral hemisphere (white arrow).

Neurological symptoms can be present in early stages of the disease and are usually characterized by seizures and development delay.

Pathogenesis

Disorders included in PROS usually carry *PIK3CA* gene mutations. The *PIK3CA* gene is responsible for encoding a subunit of PI3K that plays a critical role in the mechanistic target of rapamycin signaling pathway which is responsible, among other functions, for regulation of cell growth and proliferation.[138] Disruptions in the *PIK3CA* gene explain the growth abnormalities seen in this group of disorders, as well as some cancers associated with mutations in this gene.[132,139–141]

The *VG5Q* gene has also been described as causative for KTWS through the *t*(5;11) translocation, which results in overexpression leading to angiogenesis in several tissues.[142]

Imaging Findings

Neuroimaging findings include leptomeningeal angiomatous enhancement, intense enhancement of the choroid plexus, arteriovenous fistula, cerebral calcifications (Fig. 17B and C), cerebral atrophy, and malformations of cortical development, particularly hemimegalencephaly. Affected patients may present with cerebral hemorrhage or recurrent brain ischemia.[135,143,144] Hemimegalencephaly can be present in association with several other overgrowth disorders.[131,145]

The vascular malformations are mostly of capillary or venous origin. Arterial malformations are usually not associated with KTWS.[146]

PHACES Syndrome (OMIM 606519)

Clinical Features

PHACES syndrome represents a spectrum of abnormalities classically described as the association of posterior fossa malformation, facial hemangioma, arterial anomalies, cardiac defects/coarctation of the aorta (Fig. 18A), eye, and sternal abnormalities (Fig. 18B and C). The simultaneous coexistence of all abnormalities only occurs in a minority of cases.[147–150] PHACES has a strong female predilection with a 9:1 ratio. Diagnostic criteria have been established.[148]

Facial hemangiomas are the hallmark of PHACES syndrome, and tend to involve the trigeminal territories with a predilection for the ophthalmic segment (75%). Extracutaneous hemangiomas, including the subglottic region, are present in up to 22% of the cases. Intracranial hemangiomas (usually adjacent to the internal auditory canal) or abdominal organ involvement may occur less commonly.[147,151]

Neurological symptoms are nonspecific and include seizures, developmental delay, nystagmus, headache, and hearing impairment.[152–154]

Pathogenesis

PHACES is thought to be an X-linked dominant condition due to its female predilection.[155] It is also believed that PHACES syndrome is likely multifactorial in association with genetic predisposition, and a result of an insult early on the embryogenesis.[147,156–159]

Imaging Findings

Typical neuroimaging findings of PHACES syndrome include posterior fossa abnormalities (Fig. 18D), classically unilateral cerebellar hypoplasia and Dandy-Walker malformation, and arterial abnormalities (Fig. 18E), most commonly internal carotid artery (ICA) dysgenesis and persistence of embryonic patterns regarding origin and course of intracranial and cervical arteries. Steno-occlusive arteriopathy with a Moyamoya pattern may also be seen.[149,150,152,154,158] The

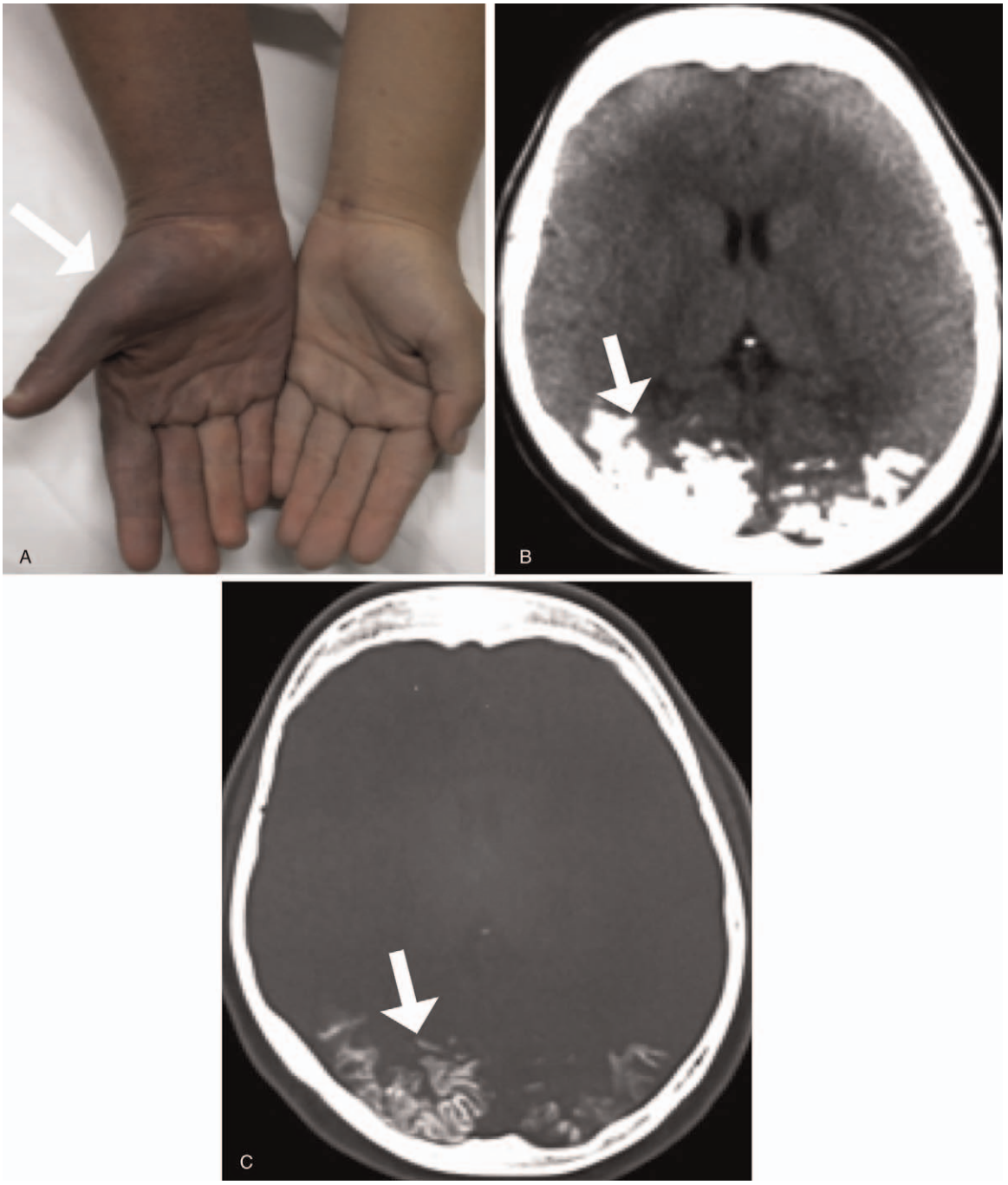

FIGURE 17. 38-Year-old woman with Klippel-Trenaunay-Weber syndrome presenting with large ''port-wine'' stain involving all divisions of the trigeminal nerves (not shown), cervical region (not shown), and the right arm (white arrow on A). Axial unenhanced CT images in brain parenchyma window (B) and osseous window (C) show gyriform calcifications on the cerebral hemispheres (white arrows).

arteriopathy seen in PHACES syndrome confers a high risk for vascular events, particularly ischemic stroke.[152]

Others imaging findings are unilateral enlargement of Meckel cave, intracranial hemangiomas, brain atrophy, malformations of cortical development, and midline defects.[152,153,158]

Reports correlate PHACES syndrome with a higher incidence of endobronchial tumors and even of glial tumors.[147,157]

Blue Rubber Bleb Syndrome (OMIM 112200)

Clinical Features

Blue rubber bleb syndrome (BRBS) is a rare vascular disorder characterized by the presence of multiple multiorgan venous malformations. Although most cases are sporadic, there have been reports of dominant, autosomal inheritance.[160,161]

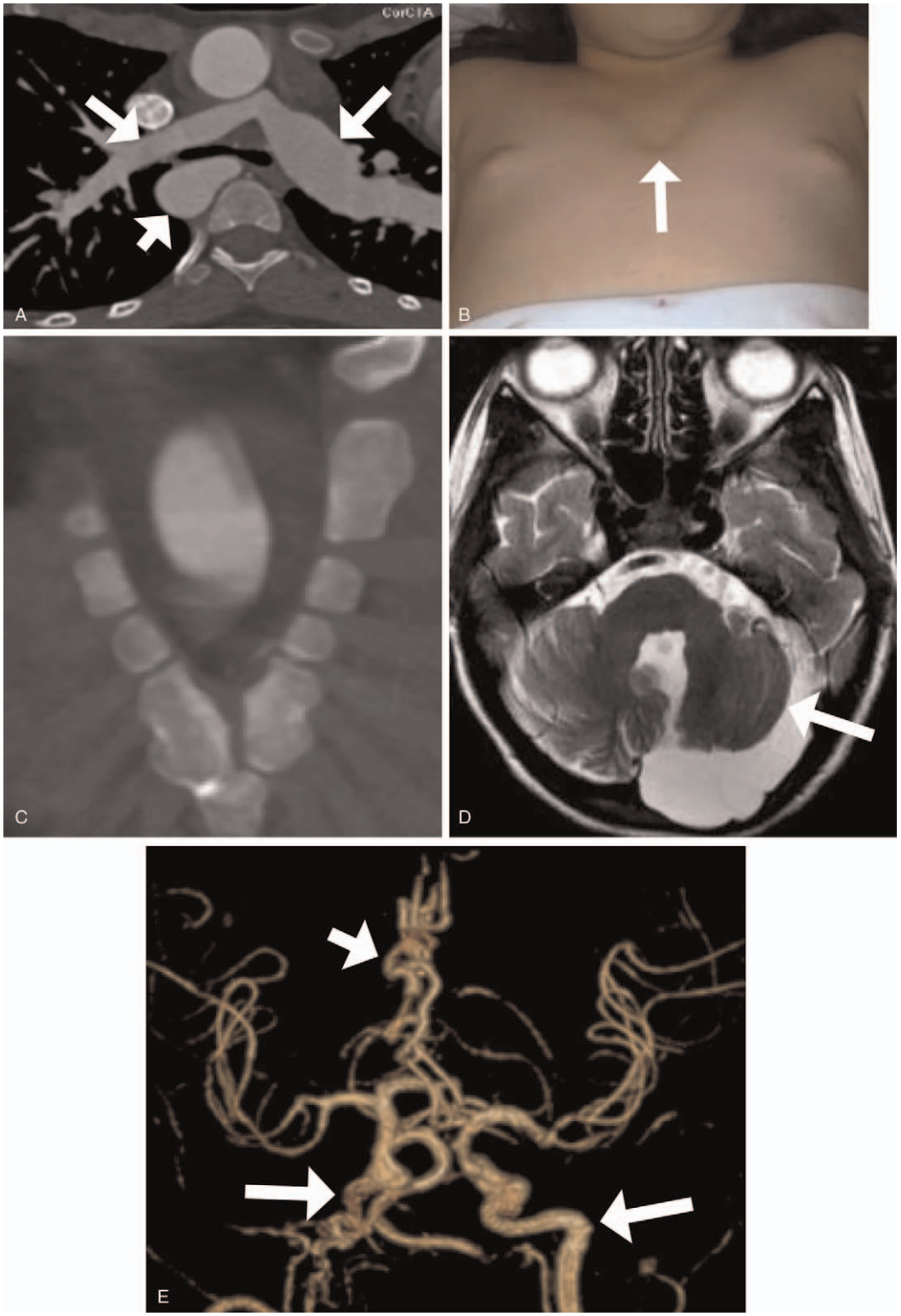

FIGURE 18. Young female child with PHACES syndrome. Axial contrast-enhanced CT (A) shows right aortic arch (short white arrow) associated with asymmetric pulmonary arteries (long white arrows) secondary to tricuspid atresia. Sternal cleft (B and C). Axial T2-weighted image (D) shows hypoplasia of the left cerebellar hemisphere associated with mega cisterna magna (white arrow). 3D image from MR angiography (E) shows ectasia of the anterior cerebral arteries (short white arrow) associated with dysplasia of the internal carotid arteries (long white arrows).

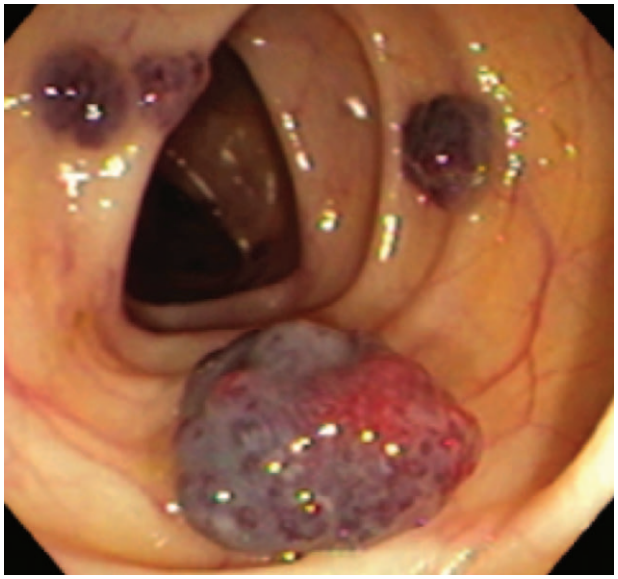

FIGURE 19. Blue rubber bleb syndrome. Colonoscopy image shows several bluish superficial lesions within the mucosa of the gastrointestinal tract, consistent with venous malformations.

Most commonly the lesions are present at birth and tend to increase in size and number with time.[160] The most common sites are the skin and gastrointestinal tract (Fig. 19), but lesions may be present in other locations, such as oropharynx and nasopharynx, abdominal organs, lung, pleura, thyroid, parotid, bone, bladder, brain, and eyes.[160,162,163]

The clinical symptoms are variable and related to the affected site, but anemia secondary to chronic intestinal bleeding is a common presentation.[162,164–167] The skin nevi are usually asymptomatic and do not require treatment.[161,165] Affected individuals carry a higher risk of developing medulloblastoma.[160]

Pathogenesis

The pathogenesis of BRBS is not fully elucidated, but the few nonsporadic cases reported are associated with the chromosome 9p.[165,168,169] Studies have proposed an association of BRBS with abnormalities in the c-kit (a stem cell growth factor receptor), and in the mTOR signaling pathway.[138,168,169] Mutation in the *TEK* gene encoding TIE2 has been reported as a cause of BRBS.[170] The *TEK* gene mediates a signaling pathway that regulates embryonic vascular development.

Imaging Findings

The CNS is rarely involved in BRBS. The disorder is characterized by the presence of multiple vascular malformations, predominantly of venous nature, such as hemangiomas, developmental venous anomalies, sinus pericranii, and capillary telangiectasias.[160,171,172] They are usually low-flow lesions, with no abnormal *flow void* seen on MRI, that most commonly present with hyperintense signal on T2-weighted images and intense homogenous enhancement after gadolinium administration (Fig. 20A, B, and C).[162,173]

Osseous abnormalities may also occur, with multiple lytic lesions and cortical remodeling secondary to the vascular malformations.[162]

OTHER PHAKOMATOSES

Basal Cell Nevus Syndrome (OMIM 109400)

Clinical Features

Basal cell nevus syndrome (BCNS), also known as Gorlin-Goltz syndrome, is a rare X-linked highly penetrant autosomal dominant disorder. It is characterized by the presence of basal cell carcinomas, odontogenic keratocysts, palmar/plantar pits and ectopic calcification of the falx cerebri, present in up to 90% of the patients.[174–176] The complete clinical spectrum may also include several craniofacial abnormalities such as macrocephaly, microcephaly, facial asymmetry, cleft lip/palate, and dental, ocular, and skeletal abnormalities (Table 3).[175,177]

The skin abnormalities may be the first clue for the correct diagnosis, typically appearing as focal dermal hypoplasia characterized by skin atrophy in areas that previously showed inflammatory/erythematous changes since birth, and later progressed to hypopigmentation with crusted erosions. Other skin abnormalities include papillomas, which are more commonly seen in the perioral area, groin and extremities, lipomatous skin changes, and patchy alopecia.[177]

Pathogenesis

BCNS is most commonly caused by mutations affecting the transmembrane protein patched homolog 1 (*PTCH1*) (50%–90% of the cases). Mutations in the protein suppressor of fused (*SUFU*) gene and in the PTCH2 also occur (15%–27% of the cases).[55,175,176,178–182] The *PTCH1* gene acts as a tumor suppression in the SHH signaling pathway, and mutations in this gene leads to functional loss of PTCH1 protein and consequent activation of the SHH signaling, which also explains the predisposition for tumorigenesis such as basal cell carcinoma and medulloblastoma.[55,175,176,183,184] BCNS is also associated with disruption of the WNT signaling cellular pathway due to a mosaicism *PORCN* mutation in the X chromosome.[185,186]

Imaging Findings

The most typical imaging findings of BCNS are odontogenic keratocysts and cerebral falx calcifications (Fig. 21A and B). The complete spectrum of imaging abnormalities includes macro- and microcephaly, skeletal abnormalities such as bifid ribs and kyphoscoliosis, and abdominal abnormalities such as hamartomas and ovarian fibromas.

Affected individuals are at a high risk of developing tumors, particularly basal cell carcinomas and keratocystic odontogenic tumors.[175,178] Neuroimaging surveillance is needed due to higher risk of intracranial tumors, especially meningiomas and SHH-activated desmoplastic medulloblastomas (Fig. 22).[55]

Encephalocraniocutaneous Lipomatosis (OMIM 613001)

Clinical Features

Encephalocraniocutaneous lipomatosis (ECCL) is a rare sporadic mesenchymal disorder with close to 100 cases reported. It affects mainly tissues of ectoderm and mesoderm origin and present with unilateral skin lesions, ocular, and CNS abnormalities.[55,187–189]

ECCL was recently included in the larger group of RASopathies and, like other disorders in this group, shows multiorgan involvement particularly of the cardiovascular, CNS, skin, and ocular systems. ECCL carries a predisposition for tumorigenesis, most typically giant cell tumors and embryonal rhabdomyosarcoma.[190]

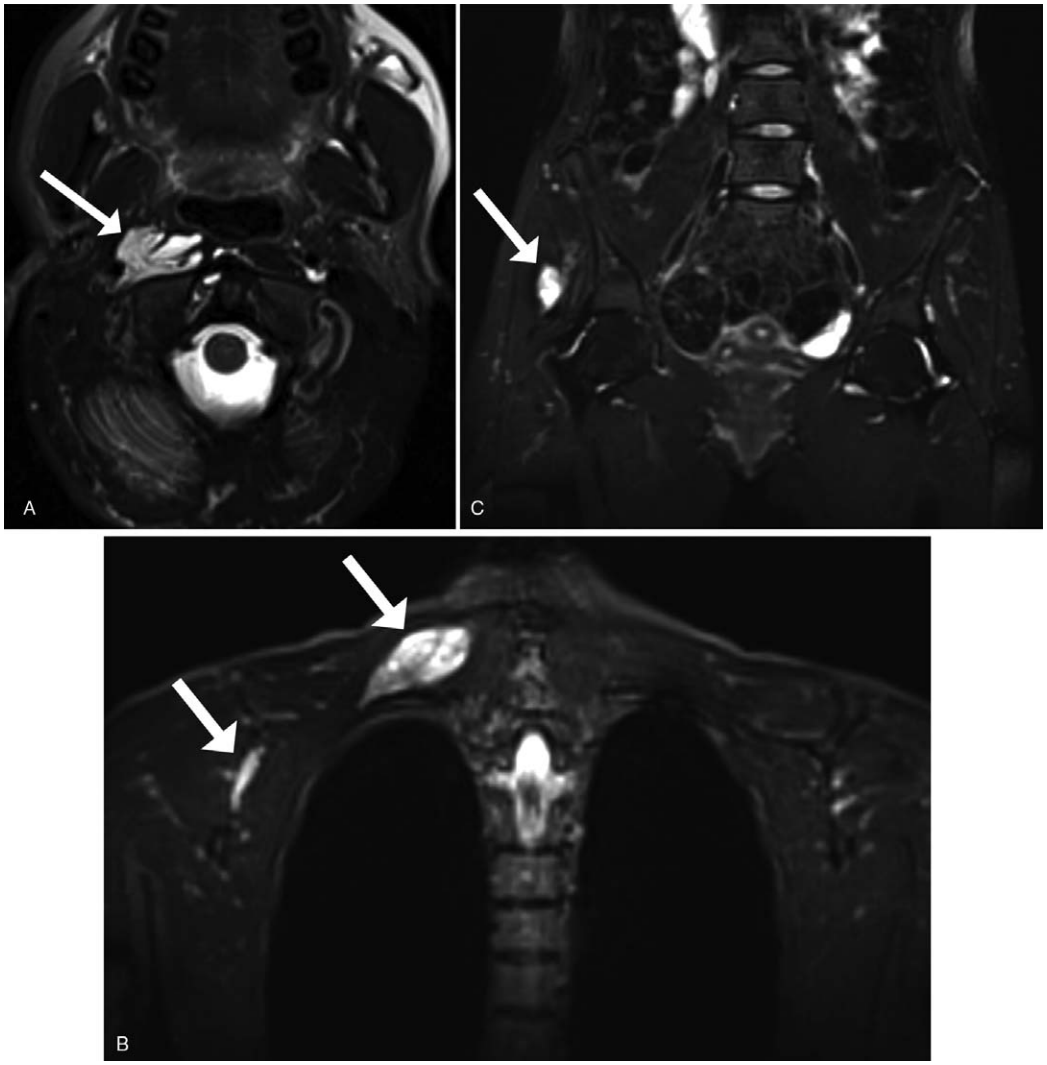

FIGURE 20. Blue rubber bleb syndrome. Axial STIR of the skull base (A), coronal STIR of the thorax (B), and pelvis (C) show several T2-hyperintense lesions consistent with venous malformations involving the right retropharyngeal space (white arrow in A) and the soft tissues of right hemithorax (white arrows in B) and pelvis (white arrow in C).

TABLE 3. Clinical Features and Neuroimaging Findings in Other Rare Phakomatoses

Other Phakomatoses	Clinical Features	Neuroimaging Findings
Gorlin-Goltz syndrome	Basal cell carcinomas, odontogenic keratocysts, focal dermal hypoplasia.	Abnormal calcification of the falx cerebri, medul loblastoma
Encephalocraniocutaneous lipomatosis	Nevus psiloliparus, subcutaneous lipomas and cafe au lait macules.	Intracranial lipoma, arachnoid cysts, inner ear abnormalities, leptomeningeal angiomatosis, cortical malformations.
Cowden-Lhermitte-Duclos syndrome	Facial trichilemmomas, acral keratosis and mucosal lesions. Overgrowth of body parts.	Cerebellar dysplastic gangliocytoma (LDD), meningioma and vascular malformations.
Bannayan-Riley-Ruvalcaba syndrome	Abnormal genital pigmentation, gastrointestinal polyps, visceral and subcutaneous lipomas, over growth of body parts.	Macrocephaly, megalencephaly, proeminent peri vascular spaces, and spinal lipomatosis.
Proteus syndrome	Overgrowth of body parts, cerebriform aspect of the connective tissue, vascular, and lymphatic malformation, with mosaic distribution that is progressive during childhood and stabilize on adolescence. Deep venous thrombosis	Hyperostosis of the external auditory meatus, macrocephaly, neuronal migration abnormalities, Dandy-Walker malformation

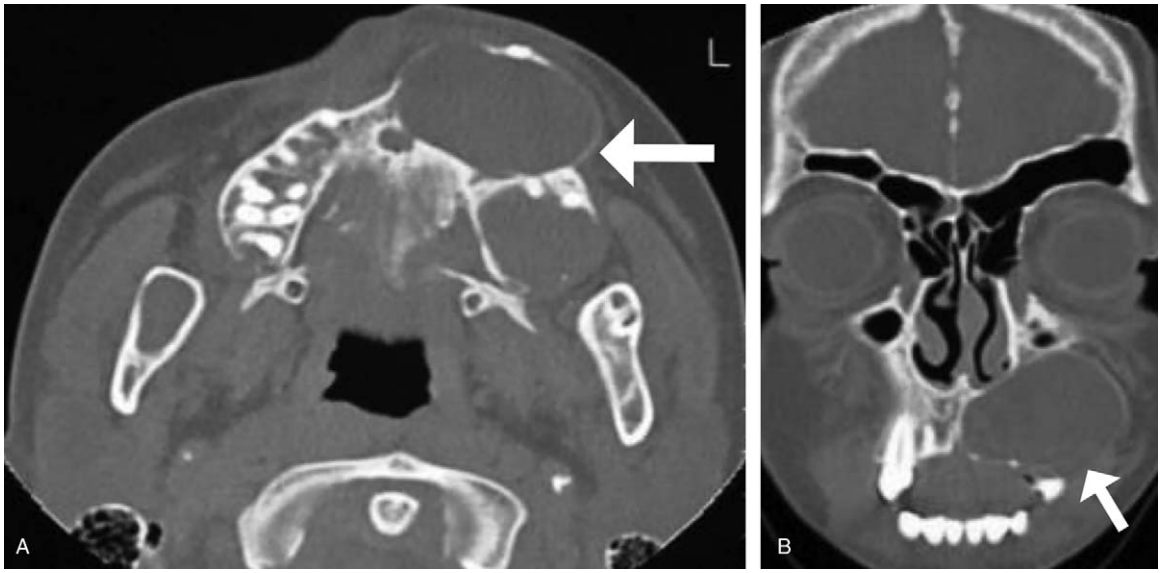

FIGURE 21. Gorlin-Goltz syndrome. Axial (A) and coronal (B) unenhanced CT images show lytic expansile lesions involving the left maxilla compatible with odontogenic keratocysts (white arrows), as well as abnormal calcification of the falx cerebri (better seen in B).

Approximately 90% of the affected patients will present with the characteristic skin change of this disorder, the nevus psiloliparus, which is characteristically located in the scalp (Fig. 23A).[187,188,191–193] Other skin abnormalities may include subcutaneous lipomas, nodular skin tags, and café-au-lait macules that follow the lines of Blaschko.[187,192]

Neurological symptoms include seizures and intellectual impairment. The level of intellectual impairment has not been correlated with the severity of the imaging findings.[55,187] Ocular abnormalities are variable, choristomas being the most common among them,[55] but the spectrum also includes colobomas, aniridia, glaucoma, microphthalmia, and calcifications.[187–189,192,193] Congenital heart defects, coarctation of the aorta, and urogenital abnormalities are also seen.

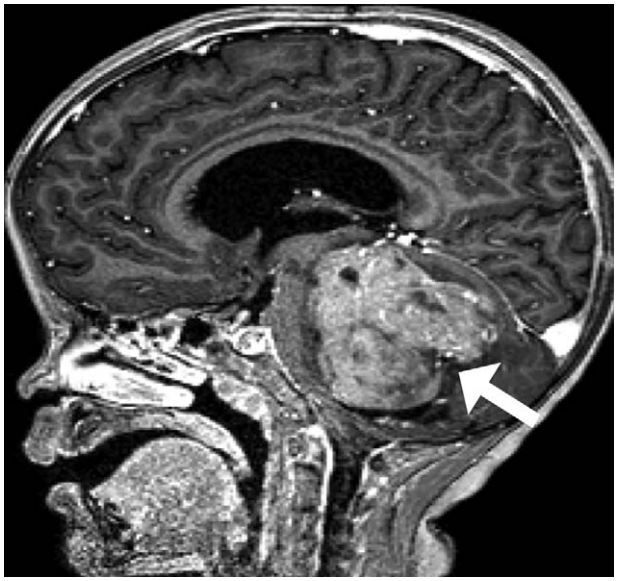

FIGURE 22. Young male child with Gorlin-Goltz syndrome and positive family history for basal cell carcinoma. Sagittal contrast-enhanced T1-weighted image shows macrocephaly associated with an intensely enhancing cerebellar mass (white arrow) compatible with medulloblastoma.

Pathogenesis

ECCL is included in the group of RASopathies, which include disorders caused by a germline mutation in genes responsible for encoding components of the MPKA (RAS-mitogen-activated protein kinase) signaling pathway, which regulates several cellular processes, such as DNA synthesis and cell growth and differentiation.[190,191] Recent data suggest that ECCL may be caused by a postzygotic somatic activating mutation in the *FGFR1* gene, located on chromosome 8p11.[191]

Imaging Findings

Imaging features of ECCL overlap with other neurocutaneous disorders. Neuroimaging findings include intracranial and intraspinal lipomas (Fig. 23B), arachnoid cysts, deficiency of the falx, hydrocephalus, corpus callosum dysgenesis, leptomeningeal angiomatosis (Fig. 23C), inner ear abnormalities, and cortical malformations (Fig. 23D), most typically hemimegalencephaly and associated facial hypertrophy. Spinal lipomatosis can also be seen with variable extension, sometimes extending throughout the entire length of the spinal canal.[55,187,188,192,194]

Other imaging findings may include skull hyperostosis, bifid ribs, mesenchymal tumors such as lipomas, choristomas, odontomas, ossifying fibromas, and benign jaw tumors such as odontomas and ossifying fibromas.[194,195] Affected patients also carry a higher risk for development of gliomas.[188]

Cowden-Lhermitte-Duclos Syndrome (OMIM 158350)

Clinical Features

Cowden-Lhermitte-Duclos syndrome (COLD) is a rare autosomal dominant hereditary disorder with multiorgan

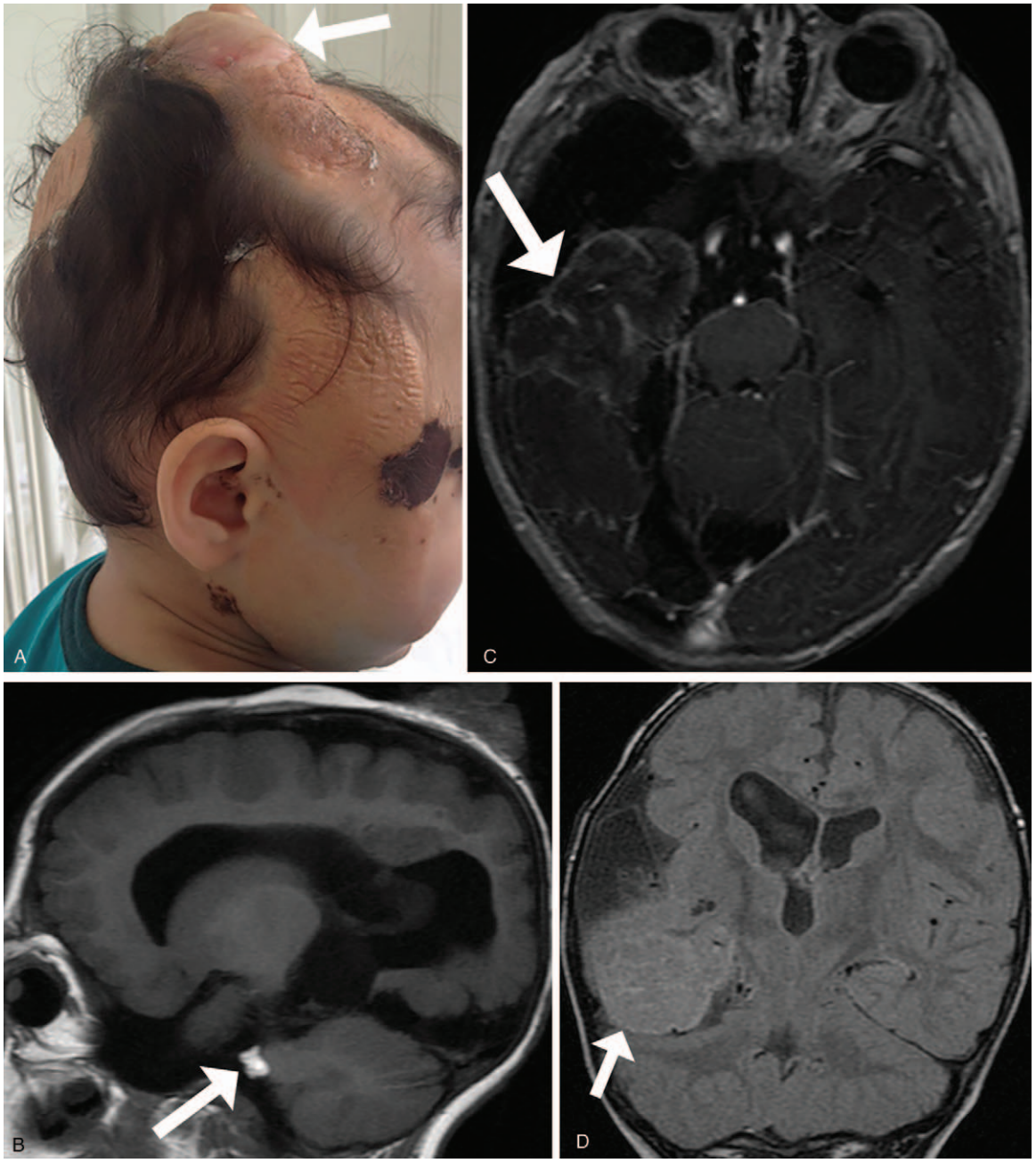

FIGURE 23. 4-Year-old boy with encephalocraniocutaneous lipomatosis. Fatty tissue nevi, smoothly surfaced and hairless involving the scalp, compatible with nevus psiloliparus (white arrow on A). Sagittal unenhanced T1-weighted image (B) shows nodular hyperintense lesion in the right cerebellopontine angle compatible with intracranial lipoma (white arrow). Axial contrast-enhanced T1-weighted image (C) shows abnormal leptomeningeal enhancement in the right temporal lobe, compatible with leptomeningeal angiomatosis (white arrow). Coronal T2-FLAIR image (D) shows cortical thickening and blurring of the grey-white matter junction as well as parenchymal signal hyperintensity, compatible with cortical dysplasia (white arrow).

involvement belonging to the group of phosphatase and tensin homolog (PTEN) hamartoma tumor syndrome (PHTS). It is characterized by the development of multiples hamartomas in different systems, and a higher rate of tumorigenesis, both benign and malignant.[196–200] The clinical spectrum of COLD is variable and overlaps with other PTEN syndromes.

Lhermitte-Duclos disease (LDD), or dysplastic gangliocytoma of the cerebellum, is a rare hamartomatous abnormality in which the classical imaging finding is a non- or slowly progressive cerebellar mass with a striped appearance that typically enlarges the interfolial space.[55,196]

The diagnosis of COLD can be made exclusively on the basis of clinical features when their pathognomonic findings are present:

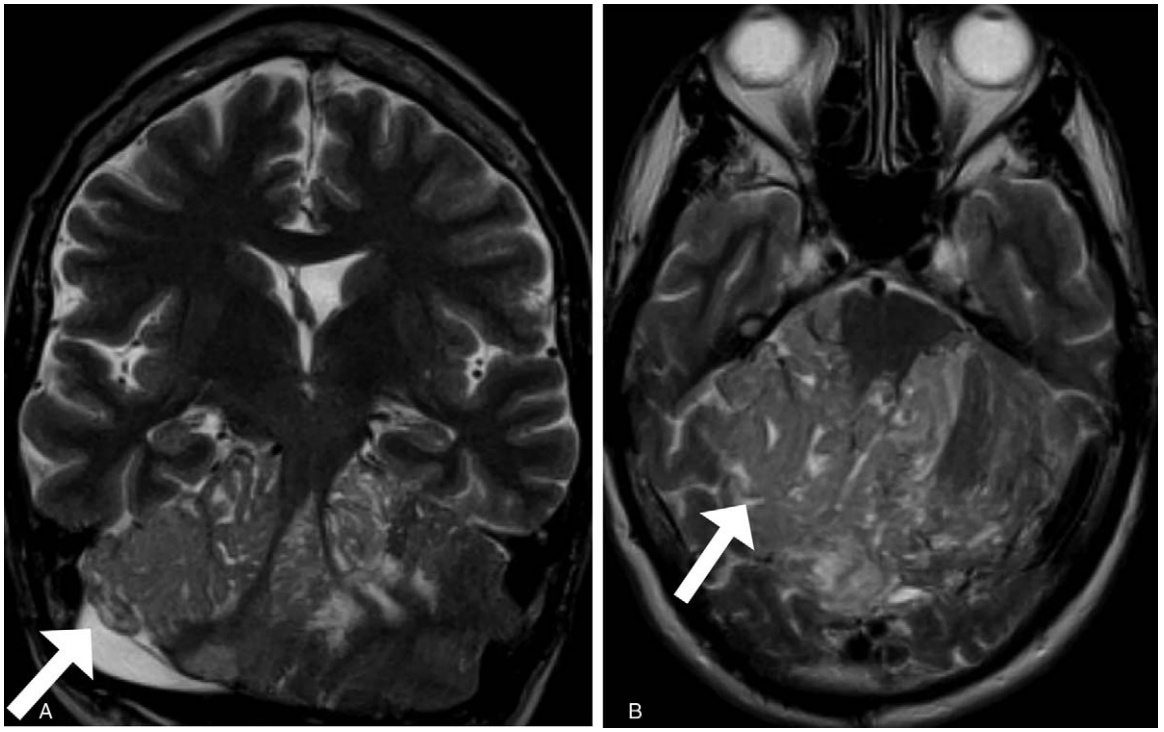

FIGURE 24. Cowden-Lhermitte-Duclos syndrome. Coronal (A) and axial (B) T2-weighted images show a hyperintense expansile cerebellar lesion with a ''tiger-striped'' appearance compatible with Lhermitte-Duclos disease (also known as desmoplastic cerebellar gangliocytoma) (white arrows).

facial trichilemmomas, acral keratosis, papillomatous papules, and mucosal lesions.[201]

The spectrum of benign tumors associated with COLD includes meningiomas, breast fibroadenomas, gastrointestinal polyps, uterine fibroids, and thyroid adenomas, among others.[196,198] All patients with COLD must be periodically screened for tumors. The most common malignancies seen in these patients involve the breast, thyroid, and endometrium. However, other malignancies can also be seen such as renal cell carcinoma, melanoma, and colon cancer.[196,202–205]

Pathogenesis

COLD is part of PHTS. It is caused by mutations in the tumor suppressor gene *PTEN*, included in the mTOR signaling pathway that regulates cellular growth and proliferation.[138,198,199,206–215] As a result, patients with PTEN-related syndromes have a higher risk of developing tumors, but the risk is particularly high in COLD.[216] Other mutations have also been identified such as germline mutation in the *SDHB*, *SDHC*, and *SHD* genes.[206]

All patients diagnosed with COLD should be tested for *PTEN* mutations, as well as their family members, due to the autosomal dominant inheritance pattern.

Imaging Findings

LDD is the most typical finding in the CNS. Its classic imaging appearance is an expansile lesion that appears isodense on CT, isointense on T1-weighted imaging and hyperintense on T2-weighted imaging, with a typical striated pattern (Fig. 24A and B). Contrast enhancement is variable, but most commonly absent.[196,197,217] Surgical resection is the treatment of choice; however, rapamycin was recently reported as an effective treatment, especially in bilateral cerebellar LDD.[196,218]

Other CNS imaging features are macrocephaly, AVMs, and hemangiomas.[197,217] The incidence of meningiomas approaches that of LDD in COLD.[200]

Bannayan-Riley-Ruvalcaba Syndrome (OMIM 153480)

Clinical Features

Bannayan-Riley-Ruvalcaba syndrome (BRRS) is a rare autosomal dominant disorder. It is caused by a germline mutation in the *PTEN* gene (involved in the mTOR signaling pathway) and is included in the group of PTEN syndromes.[138]

The clinical features are highly variable and overlapping among other neurocutaneous disorders, but affected patients usually present with multiorgan abnormalities such as macrocephaly, visceral and subcutaneous lipomas, hemangiomas, genitalia abnormalities, myopathy, pectus excavatum, scoliosis, and hamartomatous growth in several systems, mainly in the intestines, represented by polyps.[208,209,219–221]

There are no formal diagnostic criteria for BRRS, but it must be suspected when its main clinical features are present: macrocephaly, genital pigmentation abnormalities, and gastrointestinal polyps.[201,208,216]

BRRS is reported with childhood onset, as opposed to COLD, which is rarely diagnosed before adolescence.[208,209]

Neurological features are usually nonspecific and include development delay, muscular hypotonia, and seizures.[208,219] Craniofacial abnormalities are also common and include frontal bossing, downslanting palpebral fissures, strabismus, hypertelorism, depressed nasal bridge, long philtrum, epicanthus inversus, a broad mouth, and relative micrognathia.[209,221]

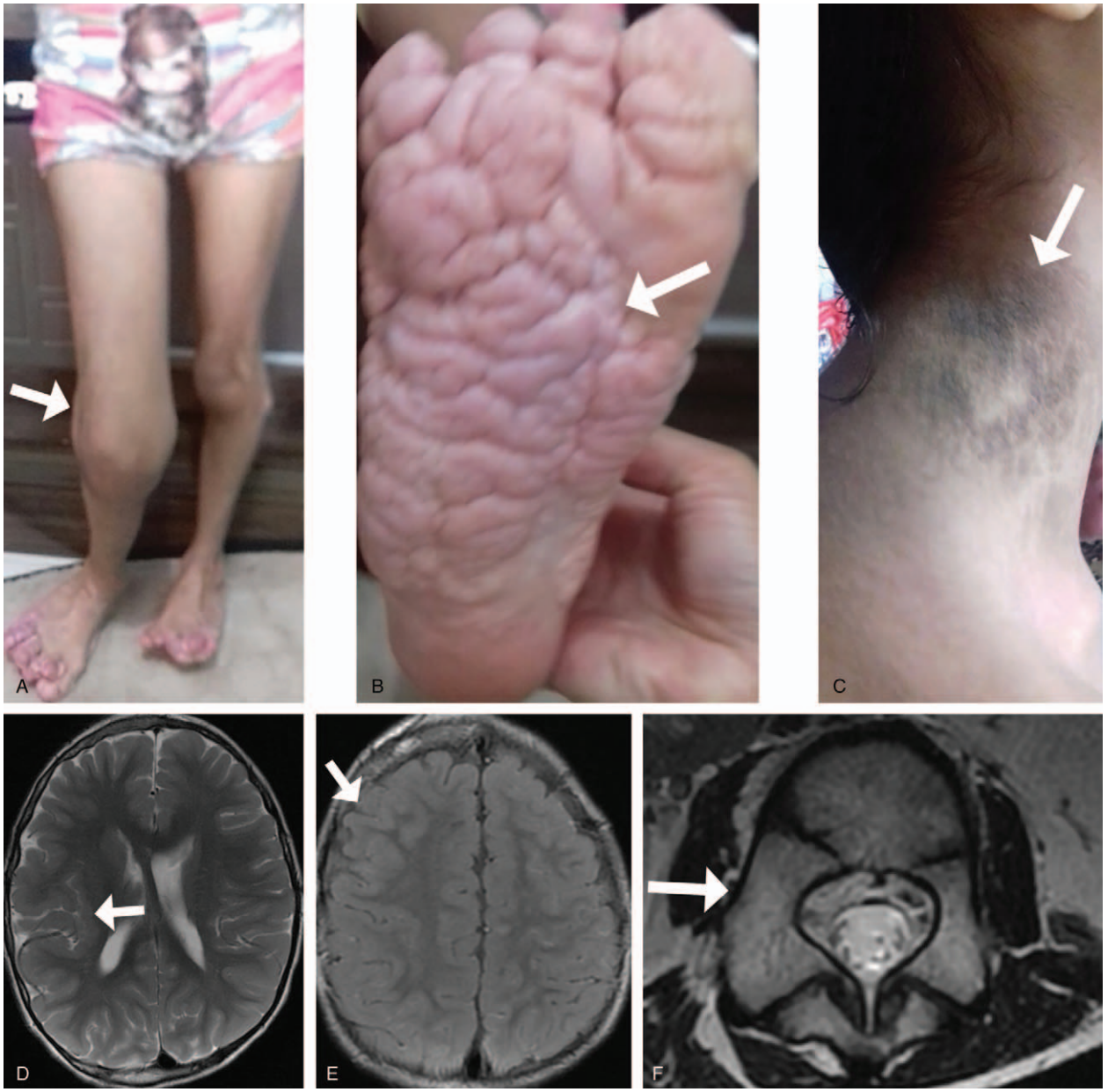

FIGURE 25. 5-Year-old girl with Proteus syndrome. Asymmetric overgrowth of the right leg (white arrow on A). Cerebriform aspect of the plantar surface of the right foot (B). Epidermal nevi on the right surface of the neck (C). Axial T2-weighted image (D) shows right perisylvian polymicrogyria (white arrow). Axial T2-FLAIR image (E) shows right hemimegalencephaly (white arrow). Axial T2-weighted image of the lumbar spine (F) shows asymmetric overgrowth of a right vertebral pedicle (white arrow).

Pathogenesis

BRRS is caused by a mutation of the *PTEN* gene, located on chromosome 10q23.3. However, this mutation is not present in all cases of BRRS.[208,209,211,214] *PTEN* mutations are present in approximately 80% of COLD, 60% of BRRS, and 20% of Proteus syndrome (PS).[208,209]

Imaging Findings

Macrocephaly and megalencephaly are prevalent, the former present in virtually all affected patients and the latter usually associated with other overgrowth features.[208] As with other PTEN syndromes, BRRS can be associated with intracranial vascular abnormalities.[208,222] Other findings include prominent perivascular spaces, intracranial, and spinal lipomatosis.[219]

Proteus Syndrome (OMIM 176920)

Clinical Features

PS syndrome is a rare disorder with an estimated prevalence of 1:1.000.000,[223] that presents with a variable spectrum of

clinical features, characterized by asymmetric overgrowth of body parts (Fig. 25A), skin abnormalities, vascular and lymphatic malformations. It presents with a mosaic distribution of the lesions that tend to be progressive during childhood and then stabilize during adolescence.[224,225]

PS may overlap with other phakomatoses, but shows some particular clinical features: cerebriform aspect of the connective tissue, more commonly seen on the plantar surfaces of the feet (Fig. 25B), thin limbs, epidermal nevi (Fig. 25C), fatty overgrowth, pulmonary abnormalities, and brain malformations.[226,227] In conjunction with the cerebriform aspect of the connective tissue, the presence of hyperostosis of the external auditory meatus is highly specific.[228]

The diagnostic criteria for PS are based on clinical features and includes the 3 main characteristics of the disorder: mosaic distribution of lesions, sporadic occurrence, and progressive course.[225] The revised diagnostic criteria divide the clinical features into 3 categories. Category A, which is the most important, includes only the cerebriform aspect of connective tissue, a highly specific finding of PS, but not always present.[226]

Affected patients are at a higher risk of neoplasms such as lipomas (most common), parotid adenomas, testicular tumors, meningiomas, and mesotheliomas. In addition, they are more susceptible to deep venous thrombosis that may be complicated by pulmonary embolism, one of the main causes of death.[225,226,229]

Neurological symptoms are nonspecific and may include development delay, intellectual disability, and seizures.

Pathogenesis

PS is thought to be associated with a mosaicism for a somatic activating mutation in the *AKT1* gene on chromosome 14q32.3, present in up to 90% of the cases.[230] There is no direct correlation between symptom severity and the proportion of mutant alleles.[230]

Imaging Findings

The imaging findings of PS are variable and nonspecific; however, the diagnosis can be suspected if presented with other clinical features. Neuroimaging findings include macrocephaly, Dandy-Walker malformation, callosal dysgenesis, and malformations of cortical development (Fig. 25D) including hemimegalencephaly (Fig. 25E). Craniofacial abnormalities including abnormal hyperostosis, craniosynostosis, and facial asymmetry may also be seen.[226]

Skeletal abnormalities are also vastly reported and include scoliosis and asymmetric overgrowth (Fig. 25F), which can lead to several complications such as spinal canal stenosis, tethered cord, and even airway obstruction.[227,231]

Abdominal organ abnormalities can also be present such as renal asymmetry, renal cysts, and hydronephrosis.[226]

In summary, the spectrum of clinical findings of melanophakomatoses, vascular phakomatoses, and other phakomatoses that may show overgrowth is vast. Many disorders share overlapping features which may pose a challenge to the diagnosis. However, a multidisciplinary approach that includes knowledge regarding imaging findings can improve the overall outcome by establishing an early diagnosis and effective therapeutic interventions. The increased understanding of the molecular basis of rare neurocutaneous disorders creates hope for the development of targeted therapies.

REFERENCES

1. Gilbert S. *Formation of the Neural Tube. Developmental Biology.* 6th ed, Sunderland: Sinauer Associates; 2000.
2. Raybaud C, Tortori-Donati P, Rossi A, et al. *Embryology of the Brain. Pediatric Neuroradiology.* Berlin, Heidelberg: Springer; 2005.
3. Steventon B, Araya C, Linker C, et al. Differential requirements of BMP and Wnt signalling during gastrulation and neurulation define two steps in neural crest induction. *Development*. 2009;136:771–779.
4. Steventon B, Mayor R. Early neural crest induction requires an initial inhibition of Wnt signals. *Dev Biol*. 2012;365:196–207.
5. Bond AM, Bhalala OG, Kessler JA. The dynamic role of bone morphogenetic proteins in neural stem cell fate and naturation. *Dev Neurobiol*. 2012;72:1068–1084.
6. Flores-Sarnat LB, Sarnat H. Embryology of neurocutaneous syndromes. In: *Neurocutaneous Disorders Phakomatoses and Hamartoneoplastic Syndromes*. Vienna: Springer; 2008. 1–17.
7. Rahimi-Movaghar V, Karimi M. Meningeal melanocytoma of the brain and oculodermal melanocytosis (nevus of Ota): case report and literature review. *Surg Neurol*. 2003;59:200–210.
8. Vezina G. Neuroimaging of phakomatoses: overview and advances. *Pediatr Radiol*. 2015;45(suppl 3):S433–S442.
9. Varshney N, Kebede AA, Owusu-Dapaah H, et al. A review of Von Hippel-Lindau syndrome. *J Kidney Cancer*. 2017;4:20–29.
10. Rosser T. Neurocutaneous disorders. *Continuum (Minneap Minn)*. 2018;24(1 Child Neurology):96–129.
11. Tragardh M, Thomsen CR, Thorninger R, et al. Hypomelanosis of Ito presenting with pediatric orthopedic issues: a case report. *J Med Case Rep*. 2014;8:156.
12. Kentab AY, Hassan HH, Hamad MH, et al. The neurologic aspects of hypomelanosis of Ito: case report and review of the literature. *Sudan J Paediatr*. 2014;14:61–70.
13. Pavone P, Pratico AD, Ruggieri M, et al. Hypomelanosis of Ito: a round on the frequency and type of epileptic complications. *Neurol Sci*. 2015;36:1173–1180.
14. Bhat RY, Patra S, Varma PV, et al. Hypomelanosis of Ito with an unusual pulmonary abnormality in an infant. *Indian Dermatol Online J*. 2014;5: 196–197.
15. Ponti G, Pellacani G, Tomasi A, et al. Hypomelanosis of Ito with a trisomy 2 mosaicism: a case report. *J Med Case Rep*. 2014;8:333.
16. Pavone V, Signorelli SS, Pratico AD, et al. Total hemi-overgrowth in pigmentary mosaicism of the (hypomelanosis of) Ito type: eight case reports. *Medicine (Baltimore)*. 2016;95:e2705.
17. Koehler M, Rouse N, Koehler TM, et al. Hypomelanosis of Ito in two infants: a case series with literature review. *Journal of the American Osteopathic College of Dermatology*. 2015;32:49–51.
18. Barbel P, Brown S, Peterson K. Identification of hypomelanosis of Ito in pediatric primary care. *J Pediatr Health Care*. 2015;29:551–554.
19. Geetha K, Priya GL, Rameshwari T. Hypomelanosis of Ito associated with cafe-au-lait spot and angiomatous nevi. *Indian J Paediatr Dermatol*. 2015;16:221–223.
20. Inoue M, Fukuda M, Ishii E, et al. Linear leukoplakia and central nervous system lesions: a clinical clue to the diagnosis of hypomelanosis of Ito. *J Pediatr*. 2015;167:771.e1.
21. Matsuzaki Y, Rokunohe A, Minakawa S, et al. Incontinentia pigmenti in a male (XY) infant with long-term follow up over 8 years. *J Dermatol*. 2018;45:100–103.
22. Soltirovska Salamon A, Lichtenbelt K, Cowan FM, et al. Clinical presentation and spectrum of neuroimaging findings in newborn infants with incontinentia pigmenti. *Dev Med Child Neurol*. 2016;58:1076–1084.
23. Greene-Roethke C. Incontinentia pigmenti: a summary review of this rare ectodermal dysplasia wth neurologic manifestations, including treatment protocols. *J Pediatr Health Care*. 2017;31:e45–e52.

24. Alabdullatif Z, Coulombe J, Steffann J, et al. Postzygotic mosaicism and incontinentia pigmenti in male patients: molecular diagnosis yield. *Br J Dermatol*. 2017;178:e261–e262.
25. Happle R. The categories of cutaneous mosaicism: a proposed classification. *Am J Med Genet A*. 2016;170A:452–459.
26. Hand JL. What's new with common genetic skin disorders? *Curr Opin Pediatr*. 2015;27:460–465.
27. Pizzamiglio MR, Piccardi L, Bianchini F, et al. Cognitive-behavioural phenotype in a group of girls from 1.2 to 12 years old with the incontinentia pigmenti syndrome: recommendations for clinical management. *Appl Neuropsychol Child*. 2017;6:327–334.
28. Conte MI, Pescatore A, Paciolla M, et al. Insight into IKBKG/NEMO locus: report of new mutations and complex genomic rearrangements leading to incontinentia pigmenti disease. *Hum Mutat*. 2014;35:165–177.
29. Ohnishi H, Kishimoto Y, Taguchi T, et al. Immunodeficiency in two female patients with incontinentia pigmenti with heterozygous NEMO mutation diagnosed by LPS unresponsiveness. *J Clin Immunol*. 2017;37:529–538.
30. Swinney CC, Han DP, Karth PA. Incontinentia pigmenti: a comprehensive review and update. *Ophthalmic Surg Lasers Imaging Retina*. 2015;46:650–657.
31. Dangouloff-Ros V, Hadj-Rabia S, Oliveira Santos J, et al. Severe neuroimaging anomalies are usually associated with random X inactivation in leucocytes circulating DNA in X-linked dominant incontinentia pigmenti. *Mol Genet Metab*. 2017;122:140–144.
32. Wolf NI, Kramer N, Harting I, et al. Diffuse cortical necrosis in a neonate with incontinentia pigmenti and an encephalitis-like presentation. *AJNR Am J Neuroradiol*. 2005;26:1580–1582.
33. Bal E, Laplantine E, Hamel Y, et al. Lack of interaction between NEMO and SHARPIN impairs linear ubiquitination and NF-kappaB activation and leads to incontinentia pigmenti. *J Allergy Clin Immunol*. 2017;140:1671.e2–1682.e2.
34. Steffann J, Raclin V, Smahi A, et al. A novel PCR approach for prenatal detection of the common NEMO rearrangement in incontinentia pigmenti. *Prenat Diagn*. 2004;24:384–388.
35. Muller K, Courtois G, Ursini MV, et al. New insight into the pathogenesis of cerebral small-vessel diseases. *Stroke*. 2017;48:520–527.
36. Poretti A, Northington FJ. Brain injury in neonatal incontinentia pigmenti: the role of multimodality neuroimaging. *Dev Med Child Neurol*. 2016;58:1000–1001.
37. Lou H, Zhang L, Xiao W, et al. Nearly completely reversible brain abnormalities in a patient with incontinentia pigmenti. *AJNR Am J Neuroradiol*. 2008;29:431–433.
38. Gocmen R, Guler E, Arslan EA. A case of neurocutaneous melanosis and neuroimaging findings. *J Radiol Case Rep*. 2015;9:1–6.
39. Kadonaga JN, Frieden IJ. Neurocutaneous melanosis: definition and review of the literature. *J Am Acad Dermatol*. 1991;24(5 pt 1):747–755.
40. Bekiesinska-Figatowska M, Sawicka E, Zak K, et al. Age related changes in brain MR appearance in the course of neurocutaneous melanosis. *Eur J Radiol*. 2016;85:1427–1431.
41. Van Engen-van Grunsven AC, Rabold K, Kusters-Vandevelde HV, et al. Copy number variations as potential diagnostic and prognostic markers for CNS melanocytic neoplasms in neurocutaneous melanosis. *Acta Neuropathol*. 2017;133:333–335. Germany.
42. Salgado CM, Basu D, Nikiforova M, et al. Amplification of mutated NRAS leading to congenital melanoma in neurocutaneous melanocytosis. *Melanoma Res*. 2015;25:453–460.
43. Kusters-Vandevelde HV, Kusters B, Van Engen-van Grunsven AC, et al. Primary melanocytic tumors of the central nervous system: a review with focus on molecular aspects. *Brain Pathol*. 2015;25:209–226.
44. Ramesh R, Shaw N, Miles EK, et al. Mosaic NRAS Q61R mutation in a child with giant congenital melanocytic naevus, epidermal naevus syndrome and hypophosphataemic rickets. *Clin Exp Dermatol*. 2017;42:75–79.
45. Kinsler VA, Thomas AC, Ishida M, et al. Multiple congenital melanocytic nevi and neurocutaneous melanosis are caused by postzygotic mutations in codon 61 of NRAS. *J Invest Dermatol*. 2013;133:2229–2236.
46. Shih F, Yip S, McDonald PJ, et al. Oncogenic codon 13 NRAS mutation in a primary mesenchymal brain neoplasm and nevus of a child with neurocutaneous melanosis. *Acta Neuropathol Commun*. 2014;2:140.
47. Van Engen-van Grunsven AC, Kusters-Vandevelde H, Groenen PJ, et al. Update on molecular pathology of cutaneous melanocytic lesions: what is new in diagnosis and molecular testing for treatment? *Front Med (Lausanne)*. 2014;1:39.
48. Uguen A, Laurent C, Samaison L, et al. Severe hydrocephalus caused by diffuse leptomeningeal and neurocutaneous melanocytosis of antenatal onset: a clinical, pathologic, and molecular study of 2 cases. *Hum Pathol*. 2015;46:1189–1196.
49. Salgado CM, Basu D, Nikiforova M, et al. BRAF mutations are also associated with neurocutaneous melanocytosis and large/giant congenital melanocytic nevi. *Pediatr Dev Pathol*. 2015;18:1–9.
50. Kusters-Vandevelde HV, Willemsen AE, Groenen PJ, et al. Experimental treatment of NRAS-mutated neurocutaneous melanocytosis with MEK162, a MEK-inhibitor. *Acta Neuropathol Commun*. 2014;2:41.
51. Markovic I, Milenkovic Z, Jovanovic M, et al. Early diagnosis of asymptomatic neurocutaneous melanosis (60 month follow-up). *Pediatr Int*. 2016;58:403–405.
52. Levy R, Lara-Corrales I. Melanocytic nevi in children: a review. *Pediatr Ann*. 2016;45:e293–e298.
53. Livingstone E, Claviez A, Spengler D, et al. Neurocutaneous melanosis: a fatal disease in early childhood. *J Clin Oncol*. 2009;27:2290–2291.
54. Chen YA, Woodley-Cook J, Sgro M, et al. Sonographic and magnetic resonance imaging findings of neurocutaneous melanosis. *Radiol Case Rep*. 2016;11:29–32.
55. Bosemani T, Huisman TA, Poretti A. Pediatric neurocutaneous syndromes with cerebellar involvement. *Neuroimaging Clin N Am*. 2016;26:417–434.
56. Hayashi M, Maeda M, Maji T, et al. Diffuse leptomeningeal hyperintensity on fluid-attenuated inversion recovery MR images in neurocutaneous melanosis. *AJNR Am J Neuroradiol*. 2004;25:138–141.
57. Monica I, Kumar LP, Uppin MS, et al. Neurocutaneous melanocytosis presenting in a teenager: a case report and review of the literature. *J Cancer Res Ther*. 2015;11:649.
58. Yan L, Di L, Weihua W, et al. A study on the clinical characteristics of treating nevus of Ota by Q-switched Nd:YAG laser. *Lasers Med Sci*. 2018;33:89–93.
59. Gerami P, Pouryazdanparast P, Vemula S, et al. Molecular analysis of a case of nevus of ota showing progressive evolution to melanoma with intermediate stages resembling cellular blue nevus. *Am J Dermatopathol*. 2010;32:301–305.
60. Patzwahl R, Landau K, Kollias SS. Atypical midface tumor complicating nevus of ota. *AJNR Am J Neuroradiol*. 2005;26:2117–2121.
61. Vivancos A, Caratu G, Matito J, et al. Genetic evolution of nevus of Ota reveals clonal heterogeneity acquiring BAP1 and TP53 mutations. *Pigment Cell Melanoma Res*. 2016;29:247–253.
62. Medel R, Vasquez L, Fernandez J, et al. Giant blue nevus: a new association to nevus of Ota. *Orbit*. 2015;34:223–228.
63. Shin D, Sinha M, Kondziolka DS, et al. Intermediate-grade meningeal melanocytoma associated with nevus of Ota: a case report and review of the literature. *Melanoma Res*. 2015;25:273–278.
64. Pan H, Wang H, Fan Y. Intracranial meningeal melanocytoma associated with nevus of Ota. *J Clin Neurosci*. 2011;18:1548–1550.

65. Buntinx-Krieg T, Ouyang J, Cartwright M. An orbital malignant melanoma arising in cellular blue nevus in a patient with nevus of Ota. *Cureus*. 2016;8:e698.
66. Elmaleh-Berges M, Baumann C, Noel-Petroff N, et al. Spectrum of temporal bone abnormalities in patients with Waardenburg syndrome and SOX10 mutations. *AJNR Am J Neuroradiol*. 2013;34:1257–1263.
67. Bogdanova-Mihaylova P, Alexander MD, Murphy RPJ, et al. Waardenburg syndrome: a rare cause of inherited neuropathy due to SOX10 mutation. *J Peripher Nerv Syst*. 2017;22:219–223.
68. Hart J, Miriyala K. Neural tube defects in Waardenburg syndrome: a case report and review of the literature. *Am J Med Genet A*. 2017;173:2472–2477.
69. Morimoto N, Mutai H, Namba K, et al. Homozygous EDNRB mutation in a patient with Waardenburg syndrome type 1. *Auris Nasus Larynx*. 2018;45:222–226.
70. Jalilian N, Tabatabaiefar MA, Bahrami T, et al. A novel pathogenic variant in the MITF gene segregating with a unique spectrum of ocular findings in an extended Iranian Waardenburg syndrome Kindred. *Mol Syndromol*. 2017;8:195–200.
71. Li H, Jin P, Hao Q, et al. Identification of a novel de novo heterozygous deletion in the SOX10 gene in Waardenburg syndrome type II using next-generation sequencing. *Genet Test Mol Biomarkers*. 2017;21:681–685.
72. Edelstein S, Naidich TP, Newton TH. The rare phakomatoses. *Neuroimaging Clin N Am*. 2004;14:185–217. vii.
73. Dumitrescu CE, Collins MT. McCune-Albright syndrome. *Orphanet J Rare Dis*. 2008;3:12.
74. Cho EK, Kim J, Yang A, et al. Clinical and endocrine characteristics and genetic analysis of Korean children with McCune-Albright syndrome: a retrospective cohort study. *Orphanet J Rare Dis*. 2016;11:113.
75. Li P, Zhang ZR, Jiang Y, et al. MR and CT findings of cyst degeneration of sphenoid bone in McCune-Albright syndrome: a case report. *Cases J*. 2009;2:9376.
76. Pierce M, Scottoline B. Neonatal McCune-Albright syndrome with survival beyond two years. *Am J Med Genet A*. 2016;170:3008–3012.
77. Agopiantz M, Journeau P, Lebon-Labich B, et al. McCune-Albright syndrome, natural history and multidisciplinary management in a series of 14 pediatric cases. *Ann Endocrinol (Paris)*. 2016;77:7–13.
78. Wood LD, Noe M, Hackeng W, et al. Patients with McCune-Albright syndrome have a broad spectrum of abnormalities in the gastrointestinal tract and pancreas. *Virchows Arch*. 2017;470:391–400.
79. Salpea P, Stratakis CA. Carney complex and McCune Albright syndrome: an overview of clinical manifestations and human molecular genetics. *Mol Cell Endocrinol*. 2014;386:85–91.
80. De Sanctis L, Galliano I, Montanari P, et al. Combining real-time COLD- and MAMA-PCR TaqMan techniques to detect and quantify R201 GNAS mutations in the McCune-Albright syndrome. *Horm Res Paediatr*. 2017;87:342–349.
81. Vasilev V, Daly AF, Thiry A, et al. McCune-Albright syndrome: a detailed pathological and genetic analysis of disease effects in an adult patient. *J Clin Endocrinol Metab*. 2014;99:E2029–E2038.
82. Thomas AC, Zeng Z, Riviere JB, et al. Mosaic activating mutations in GNA11 and GNAQ are associated with phakomatosis pigmentovascularis and extensive dermal melanocytosis. *J Invest Dermatol*. 2016;136:770–778.
83. Ferreira EC, Brito CC, Domingues RC, et al. Whole-body MR imaging for the evaluation of McCune-Albright syndrome. *J Magn Reson Imaging*. 2010;31:706–710.
84. Peterson J. Hereditary hemorrhagic telangiectasia management. *Radiol Technol*. 2017;88:277–294.
85. McDonald J, Wooderchak-Donahue W, VanSant Webb C, et al. Hereditary hemorrhagic telangiectasia: genetics and molecular diagnostics in a new era. *Front Genet*. 2015;6:1.
86. Latino GA, Kim H, Nelson J, et al. Severity score for hereditary hemorrhagic telangiectasia. *Orphanet J Rare Dis*. 2014;9:188.
87. Shovlin CL, Guttmacher AE, Buscarini E, et al. Diagnostic criteria for hereditary hemorrhagic telangiectasia (Rendu-Osler-Weber syndrome). *Am J Med Genet*. 2000;91:66–67.
88. Mu W, Cordner ZA, Yuqi Wang K, et al. Characterization of pulmonary arteriovenous malformations in ACVRL1 versus ENG mutation carriers in hereditary hemorrhagic telangiectasia. *Genet Med*. 2018;20:639–644.
89. Rattani A, Dewan MC, Hannig V, et al. Cerebral hemorrhage in monozygotic twins with hereditary hemorrhagic telangiectasia: case report and hemorrhagic risk evaluation. *J Neurosurg Pediatr*. 2017;20:164–169.
90. Komiyama M. Pathogenesis of brain arteriovenous malformations. *Neurol Med Chir (Tokyo)*. 2016;56:317–325.
91. Labeyrie PE, Courtheoux P, Babin E, et al. Neurological involvement in hereditary hemorrhagic telangiectasia. *J Neuroradiol*. 2016;43:236–245.
92. Niimi Y, Uchiyama N, Elijovich L, et al. Spinal arteriovenous metameric syndrome: clinical manifestations and endovascular management. *AJNR Am J Neuroradiol*. 2013;34:457–463.
93. Kim H, Nelson J, Krings T, et al. Hemorrhage rates from brain arteriovenous malformation in patients with hereditary hemorrhagic telangiectasia. *Stroke*. 2015;46:1362–1364.
94. Garcia de Vinuesa A, Abdelilah-Seyfried S, Knaus P, et al. BMP signaling in vascular biology and dysfunction. *Cytokine Growth Factor Rev*. 2016;27:65–79.
95. Morrell NW, Bloch DB, ten Dijke P, et al. Targeting BMP signalling in cardiovascular disease and anaemia. *Nat Rev Cardiol*. 2016;13:106–120.
96. Revuz S, Decullier E, Ginon I, et al. Pulmonary hypertension subtypes associated with hereditary haemorrhagic telangiectasia: haemodynamic profiles and survival probability. *PLoS One*. 2017;12:e0184227.
97. Vorselaars VMM, Diederik A, Prabhudesai V, et al. SMAD4 gene mutation increases the risk of aortic dilation in patients with hereditary haemorrhagic telangiectasia. *Int J Cardiol*. 2017;245:114–118.
98. Roman BL, Hinck AP. ALK1 signaling in development and disease: new paradigms. *Cell Mol Life Sci*. 2017;74:4539–4560.
99. Krings T, Kim H, Power S, et al. Neurovascular manifestations in hereditary hemorrhagic telangiectasia: imaging features and genotype-phenotype correlations. *AJNR Am J Neuroradiol*. 2015;36:863–870.
100. Iodice A, Galli J, Molinaro A, et al. Neurovisual assessment in children with ataxia telangiectasia. *Neuropediatrics*. 2018;49:26–34.
101. Nissenkorn A, Ben-Zeev B. Ataxia telangiectasia. *Handb Clin Neurol*. 2015;132:199–214.
102. Zaki-Dizaji M, Akrami SM, Abolhassani H, et al. Ataxia telangiectasia syndrome: moonlighting ATM. *Expert Rev Clin Immunol*. 2017;13:1155–1172.
103. Rothblum-Oviatt C, Wright J, Lefton-Greif MA, et al. Ataxia telangiectasia: a review. *Orphanet J Rare Dis*. 2016;11:159.
104. Beaudin M, Klein CJ, Rouleau GA, et al. Systematic review of autosomal recessive ataxias and proposal for a classification. *Cerebellum Ataxias*. 2017;4:3.
105. Moin M, Aghamohammadi A, Kouhi A, et al. Ataxia-telangiectasia in Iran: clinical and laboratory features of 104 patients. *Pediatr Neurol*. 2007;37:21–28.
106. Kumar V, Alt FW, Oksenych V. Functional overlaps between XLF and the ATM-dependent DNA double strand break response. *DNA Repair (Amst)*. 2014;16:11–22.
107. Shabestari MS, Maljaei SH, Baradaran R, et al. Distribution of primary immunodeficiency diseases in the Turk ethnic group, living in the northwestern Iran. *J Clin Immunol*. 2007;27:510–516.

108. Telatar M, Teraoka S, Wang Z, et al. Ataxia-telangiectasia: identification and detection of founder-effect mutations in the ATM gene in ethnic populations. *Am J Hum Genet*. 1998;62:86–97.
109. Stell R, Bronstein AM, Plant GT, et al. Ataxia telangiectasia: a reappraisal of the ocular motor features and their value in the diagnosis of atypical cases. *Mov Disord*. 1989;4:320–329.
110. Shiloh Y, Lederman HM. Ataxia-telangiectasia (A-T): an emerging dimension of premature ageing. *Ageing Res Rev*. 2017;33:76–88.
111. Ambrose M, Gatti RA. Pathogenesis of ataxia-telangiectasia: the next generation of ATM functions. *Blood*. 2013;121:4036–4045.
112. Mortaz E, Marashian SM, Ghaffaripour H, et al. A new ataxia-telangiectasia mutation in an 11-year-old female. *Immunogenetics*. 2017;69:415–419.
113. Van Os NJ, Roeleveld N, Weemaes CM, et al. Health risks for ataxia-telangiectasia mutated heterozygotes: a systematic review, meta-analysis and evidence-based guideline. *Clin Genet*. 2016;90:105–117.
114. Savitsky K, Bar-Shira A, Gilad S, et al. A single ataxia telangiectasia gene with a product similar to PI-3 kinase. *Science*. 1995;268:1749–1753.
115. Cremona CA, Behrens A. ATM signalling and cancer. *Oncogene*. 2014;33:3351–3360.
116. Woods CG, Taylor AM. Ataxia telangiectasia in the British Isles: the clinical and laboratory features of 70 affected individuals. *Q J Med*. 1992;82:169–179.
117. Morio T, Takahashi N, Watanabe F, et al. Phenotypic variations between affected siblings with ataxia-telangiectasia: ataxia-telangiectasia in Japan. *Int J Hematol*. 2009;90:455–462.
118. Sahama I, Sinclair K, Pannek K, et al. Radiological imaging in ataxia telangiectasia: a review. *Cerebellum*. 2014;13:521–530.
119. Ruggieri M, Pratico AD. Mosaic neurocutaneous disorders and their causes. *Semin Pediatr Neurol*. 2015;22:207–233.
120. Schmidt D, Pache M, Schumacher M. The congenital unilateral retinocephalic vascular malformation syndrome (bonnet-dechaume-blanc syndrome or Wyburn-Mason syndrome): review of the literature. *Surv Ophthalmol*. 2008;53:227–249.
121. Bhattacharya JJ, Luo CB, Suh DC, et al. Wyburn-Mason or Bonnet-Dechaume-Blanc as cerebrofacial arteriovenous metameric syndromes (CAMS). A new concept and a new classification. *Interv Neuroradiol*. 2001;7:5–17.
122. Dayani PN, Sadun AA. A case report of Wyburn-Mason syndrome and review of the literature. *Neuroradiology*. 2007;49:445–456.
123. Lester J, Ruano-Calderon LA, Gonzalez-Olhovich I. Wyburn-Mason syndrome. *J Neuroimaging*. 2005;15:284–285.
124. Vanaman MJ, Hervey-Jumper SL, Maher CO. Pediatric and inherited neurovascular diseases. *Neurosurg Clin N Am*. 2010;21:427–441.
125. Pal P, Ray S, Chakraborty S, et al. Cobb syndrome: arare cause of paraplegia. *Ann Neurosci*. 2015;22:191–193.
126. Komiyama M, Ishiguro T, Terada A, et al. Spinal arteriovenous metameric syndrome in a neonate presenting with congestive heart failure: case report. *Childs Nerv Syst*. 2014;30:1607–1611.
127. Matsui Y, Mineharu Y, Satow T, et al. Coexistence of multiple cavernous angiomas in the spinal cord and skin: a unique case of Cobb syndrome. *J Neurosurg Spine*. 2014;20:142–147.
128. Abtahi-Naeini B, Saffaei A, Pourazizi M. Unusual cause of lower extremity wounds: Cobb syndrome. *Int Wound J*. 2016;13:1009–1010.
129. Schirmer CM, Hwang SW, Riesenburger RI, et al. Obliteration of a metameric spinal arteriovenous malformation (Cobb syndrome) using combined endovascular embolization and surgical excision. *J Neurosurg Pediatr*. 2012;10:44–49.
130. Clark MT, Brooks EL, Chong W, et al. Cobb syndrome: a case report and systematic review of the literature. *Pediatr Neurol*. 2008;39:423–425.
131. Oduber CE, Van der Horst CM, Hennekam RC. Klippel-Trenaunay syndrome: diagnostic criteria and hypothesis on etiology. *Ann Plast Surg*. 2008;60:217–223.
132. Vahidnezhad H, Youssefian L, Uitto J. Klippel-Trenaunay syndrome belongs to the PIK3CA-related overgrowth spectrum (PROS). *Exp Dermatol*. 2016;25:17–19.
133. Hershkovitz D, Bergman R, Sprecher E. A novel mutation in RASA1 causes capillary malformation and limb enlargement. *Arch Dermatol Res*. 2008;300:385–388.
134. Yazaki M, Kaneko K, Tojo K, et al. An unusual case of Klippel-Trenaunay-Weber syndrome presenting with portosystemic encephalopathy. *Intern Med*. 2008;47:1621–1625.
135. Uller W, Fishman SJ, Alomari AI. Overgrowth syndromes with complex vascular anomalies. *Semin Pediatr Surg*. 2014;23:208–215.
136. Sakaguchi Y, Takenouchi T, Uehara T, et al. Co-occurrence of Sturge-Weber syndrome and Klippel-Trenaunay-Weber syndrome phenotype: consideration of the historical aspect. *Am J Med Genet A*. 2017;173:2831–2833.
137. Dorairaj S, Ritch R. Encephalotrigeminal angiomatosis (Sturge-Weber syndrome, Klippel-Trenaunay-Weber syndrome): a review. *Asia Pac J Ophthalmol (Phila)*. 2012;1:226–234.
138. Shrot S, Hwang M, Stafstrom CE, et al. Dysplasia and overgrowth: magnetic resonance imaging of pediatric brain abnormalities secondary to alterations in the mechanistic target of rapamycin pathway. *Neuroradiology*. 2018;60:137–150.
139. Luks VL, Kamitaki N, Vivero MP, et al. Lymphatic and other vascular malformative/overgrowth disorders are caused by somatic mutations in PIK3CA. *J Pediatr*. 2015;166:1048.e1-5–1054.e1-e5.
140. Dimopoulos A, Sicko RJ, Kay DM, et al. Copy number variants in a population-based investigation of Klippel-Trenaunay syndrome. *Am J Med Genet A*. 2017;173:352–359.
141. Wetzel-Strong SE, Detter MR, Marchuk DA. The pathobiology of vascular malformations: insights from human and model organism genetics. *J Pathol*. 2017;241:281–293.
142. Hu Y, Li L, Seidelmann SB, et al. Identification of association of common AGGF1 variants with susceptibility for Klippel-Trenaunay syndrome using the structure association program. *Ann Hum Genet*. 2008;72(pt 5):636–643.
143. Renard D, Larue A, Taieb G, et al. Recurrent cerebral infarction in Klippel-Trenaunay-Weber syndrome. *Clin Neurol Neurosurg*. 2012;114:1019–1020.
144. Beume LA, Fuhrmann SC, Reinhard M, et al. Coincidence of ischemic stroke and recurrent brain haemorrhage in a patient with Klippel-Trenaunay syndrome. *J Clin Neurosci*. 2013;20:1454–1455.
145. Esmailzadeh H, Tavassoli A, Jahangiri NY, et al. Klippel-trenaunay-weber syndrome with hemimegalencephaly; report of a pediatric case. *Iran J Pediatr*. 2012;22:147–151.
146. Chen D, Li L, Tu X, et al. Functional characterization of Klippel-Trenaunay syndrome gene AGGF1 identifies a novel angiogenic signaling pathway for specification of vein differentiation and angiogenesis during embryogenesis. *Hum Mol Genet*. 2013;22:963–976.
147. Mama N, H'Mida D, Lahmar I, et al. PHACES syndrome associated with carcinoid endobronchial tumor. *Pediatr Radiol*. 2014;44:621–624.
148. Metry D, Heyer G, Hess C, et al. Consensus statement on diagnostic criteria for PHACE syndrome. *Pediatrics*. 2009;124:1447–1456.
149. Jack AS, Chow MM, Fiorillo L, et al. Bilateral pial synangiosis in a child with PHACE syndrome. *J Neurosurg Pediatr*. 2016;17:70–75.
150. Hartemink DA, Chiu YE, Drolet BA, et al. PHACES syndrome: a review. *Int J Pediatr Otorhinolaryngol*. 2009;73:181–187.
151. Judd CD, Chapman PR, Koch B, et al. Intracranial infantile hemangiomas associated with PHACE syndrome. *AJNR Am J Neuroradiol*. 2007;28:25–29.

152. Garzon MC, Epstein LG, Heyer GL, et al. PHACE syndrome: consensus-derived diagnosis and care recommendations. *J Pediatr*. 2016;178:24.e2–33.e2.
153. Wright JN, Wycoco V. Asymmetric Meckel cave enlargement: a potential marker of PHACES syndrome. *AJNR Am J Neuroradiol*. 2017;38:1223–1227.
154. Oza VS, Wang E, Berenstein A, et al. PHACES association: a neuroradiologic review of 17 patients. *AJNR Am J Neuroradiol*. 2008;29:807–813.
155. Levin JH, Kaler SG. Non-random maternal X-chromosome inactivation associated with PHACES. *Clin Genet*. 2007;72:345–350.
156. Mitchell S, Siegel DH, Shieh JT, et al. Candidate locus analysis for PHACE syndrome. *Am J Med Genet A*. 2012;158a:1363–1367.
157. Mohebali J, Walsh MT, Couldwell WT. Brainstem glioma in PHACES syndrome: case report and review of the literature. *Cent Eur Neurosurg*. 2011;72:46–48.
158. Hess CP, Fullerton HJ, Metry DW, et al. Cervical and intracranial arterial anomalies in 70 patients with PHACE syndrome. *AJNR Am J Neuroradiol*. 2010;31:1980–1986.
159. Patil SJ, Moray AA, Kiran VS, et al. PHACE/S syndrome: a syndromic infantile segmental hemangioma. *Indian J Pediatr*. 2010;77:911–913.
160. Carvalho S, Barbosa V, Santos N, et al. Blue rubber-bleb nevus syndrome: report of a familial case with a dural arteriovenous fistula. *AJNR Am J Neuroradiol*. 2003;24:1916–1918.
161. Giao Antunes AS, Peixe B, Guerreiro H. Blue rubber bleb nevus syndrome: a delayed diagnosis. *GE Port J Gastroenterol*. 2017;24:101–103.
162. Kassarjian A, Fishman SJ, Fox VL, et al. Imaging characteristics of blue rubber bleb nevus syndrome. *AJR Am J Roentgenol*. 2003;181:1041–1048.
163. Gonzalez-Hernandez J, Lizardo-Sanchez L. An atypical presentation of blue rubber bleb nevus syndrome. *Proc (Bayl Univ Med Cent)*. 2016;29:323–324.
164. Petek B, Jones RL. The management of ophthalmic involvement in blue rubber bleb nevus syndrome. *GMS Ophthalmol Cases*. 2014;4:Doc04.
165. Jin XL, Wang ZH, Xiao XB, et al. Blue rubber bleb nevus syndrome: a case report and literature review. *World J Gastroenterol*. 2014;20:17254–17259.
166. Sangwan A, Kaur S, Jain VK, et al. Blue rubber bleb nevus syndrome: a rare multisystem affliction. *Dermatol Online J*. 2015;21.
167. Lybecker MB, Stawowy M, Clausen N. Blue rubber bleb naevus syndrome: a rare cause of chronic occult blood loss and iron deficiency anaemia. *BMJ Case Rep*. 2016;2016.
168. Menegozzo CAM, Novo F, Mori ND, et al. Postoperative disseminated intravascular coagulation in a pregnant patient with Blue Rubber Bleb Nevus Syndrome presenting with acute intestinal obstruction: case report and literature review. *Int J Surg Case Rep*. 2017;39:235–238.
169. Bahl A, Raghavan A, Sinha S. Blue rubber bleb naevus syndrome and Chiari malformation: high risk of peroperative haemorrhage. *Turk Neurosurg*. 2013;23:818–820.
170. Soblet J, Kangas J, Natynki M, et al. Blue rubber bleb nevus (BRBN) syndrome is caused by somatic TEK (TIE2) mutations. *J Invest Dermatol*. 2017;137:207–216.
171. Elsayes KM, Menias CO, Dillman JR, et al. Vascular malformation and hemangiomatosis syndromes: spectrum of imaging manifestations. *AJR Am J Roentgenol*. 2008;190:1291–1299.
172. Wynford-Thomas R, Johnston A, Halpin S, et al. Rarities in neurology: blue rubber bleb naevus syndrome. *Pract Neurol*. 2014;14:360–362.
173. Kondziella D, Nordanstig A, Molne L, et al. Neurological picture: cranial neuropathy in the blue rubber bleb nevus syndrome. *J Neurol Neurosurg Psychiatry*. 2010;81:1207–1208.
174. Bronoosh P, Shakibafar AR, Houshyar M, et al. Imaging findings in a case of Gorlin-Goltz syndrome: a survey using advanced modalities. *Imaging Sci Dent*. 2011;41:171–175.
175. Onodera S, Saito A, Hasegawa D, et al. Multi-layered mutation in hedgehog-related genes in Gorlin syndrome may affect the phenotype. *PLoS One*. 2017;12:e0184702.
176. Huq AJ, Bogwitz M, Gorelik A, et al. Cohort study of Gorlin syndrome with emphasis on standardised phenotyping and quality of life assessment. *Intern Med J*. 2017;47:664–673.
177. Fete TJ, Fete M. International research symposium on Goltz syndrome. *Am J Med Genet C Semin Med Genet*. 2016;172C:3–6.
178. Morita K, Naruto T, Tanimoto K, et al. Simultaneous detection of both single nucleotide variations and copy number alterations by next-generation sequencing in Gorlin syndrome. *PLoS One*. 2015;10:e0140480.
179. Kato C, Fujii K, Arai Y, et al. Nevoid basal cell carcinoma syndrome caused by splicing mutations in the PTCH1 gene. *Fam Cancer*. 2017;16:131–138.
180. Alonso N, Canueto J, Ciria S, et al. Novel clinical and molecular findings in Spanish patients with naevoid basal cell carcinoma syndrome. *Br J Dermatol*. 2017;178:198–206.
181. Gloude NJ, Yoon JM, Crawford JR. Novel PTCH1 mutation in a young child with Gorlin syndrome and medulloblastoma. *Pediatr Blood Cancer*. 2016;63:1128–1129.
182. Ikemoto Y, Takayama Y, Fujii K, et al. Somatic mosaicism containing double mutations in PTCH1 revealed by generation of induced pluripotent stem cells from nevoid basal cell carcinoma syndrome. *J Med Genet*. 2017;54:579–584.
183. Mangum R, Varga E, Boue DR, et al. SHH desmoplastic/nodular medulloblastoma and Gorlin syndrome in the setting of Down syndrome: case report, molecular profiling, and review of the literature. *Childs Nerv Syst*. 2016;32:2439–2446.
184. Matsudate Y, Naruto T, Hayashi Y, et al. Targeted exome sequencing and chromosomal microarray for the molecular diagnosis of nevoid basal cell carcinoma syndrome. *J Dermatol Sci*. 2017;86:206–211.
185. Happle R. Goltz syndrome and PORCN: a view from Europe. *Am J Med Genet C Semin Med Genet*. 2016;172C:21–23.
186. Liu W, Shaver TM, Balasa A, et al. Deletion of Porcn in mice leads to multiple developmental defects and models human focal dermal hypoplasia (Goltz syndrome). *PLoS One*. 2012;7:e32331.
187. Michael GA, Poretti A, Huisman TA. Neuroimaging findings in encephalocraniocutaneous lipomatosis. *Pediatr Neurol*. 2015;53:462–463.
188. Kocak O, Yarar C, Carman KB. Encephalocraniocutaneous lipomatosis, a rare neurocutaneous disorder: report of additional three cases. *Childs Nerv Syst*. 2016;32:559–562.
189. Banta J, Beasley K, Kobayashi T, et al. Encephalocraniocutaneous lipomatosis (Haberland syndrome): a mild case with bilateral cutaneous and ocular involvement. *JAAD Case Rep*. 2016;2:150–152.
190. Boppudi S, Bogershausen N, Hove HB, et al. Specific mosaic KRAS mutations affecting codon 146 cause oculoectodermal syndrome and encephalocraniocutaneous lipomatosis. *Clin Genet*. 2016;90:334–342.
191. Bennett JT, Tan TY, Alcantara D, et al. Mosaic activating mutations in FGFR1 cause encephalocraniocutaneous lipomatosis. *Am J Hum Genet*. 2016;98:579–587.
192. Radic Nisevic J, Prpic I, Antulov R, et al. Encephalocraniocutaneous lipomatosis without ocular malformations. *Pediatr Neurol*. 2016;60:71–74.
193. Siddiqui S, Naaz S, Ahmad M, et al. Encephalocraniocutaneous lipomatosis: a case report with review of literature. *Neuroradiol J*. 2017;30:578–582.
194. Moog U, Jones MC, Viskochil DH, et al. Brain anomalies in encephalocraniocutaneous lipomatosis. *Am J Med Genet A*. 2007;143a:2963–2972.
195. Jain P, Chakrabarty B, Kumar A, et al. Encephalocraniocutaneous lipomatosis with neurocutaneous melanosis. *J Child Neurol*. 2014;29:846–849.

196. Jiang T, Wang J, Du J, et al. Lhermitte-Duclos disease (dysplastic gangliocytoma of the cerebellum) and Cowden syndrome: clinical experience from a single institution with long-term follow-up. *World Neurosurg*. 2017;104:398–406.

197. Gammon A, Jasperson K, Champine M. Genetic basis of Cowden syndrome and its implications for clinical practice and risk management. *Appl Clin Genet*. 2016;9:83–92.

198. Hu ZI, Bangiyev L, Seidman RJ, et al. Dysphagia and neck swelling in a case of undiagnosed Lhermitte-Duclos disease and Cowden syndrome. *Case Rep Oncol Med*. 2015;2015:546297.

199. Stepniak I, Trojanowski T, Drelich-Zbroja A, et al. Cowden syndrome and the associated Lhermitte-Duclos disease—case presentation. *Neurol Neurochir Pol*. 2015;49:339–343.

200. Yakubov E, Ghoochani A, Buslei R, et al. Hidden association of Cowden syndrome, PTEN mutation and meningioma frequency. *Oncoscience*. 2016;3:149–155.

201. Sagi SV, Ballard DD, Marks RA, et al. Bannayan Ruvalcaba Riley syndrome. *ACG Case Rep J*. 2014;1:90–92.

202. Derrey S, Proust F, Debono B, et al. Association between Cowden syndrome and Lhermitte-Duclos disease: report of two cases and review of the literature. *Surg Neurol*. 2004;61:447–454.

203. Riegert-Johnson DL, Gleeson FC, Roberts M, et al. Cancer and Lhermitte-Duclos disease are common in Cowden syndrome patients. *Hered Cancer Clin Pract*. 2010;8:6.

204. Yu W, Ni Y, Saji M, et al. Cowden syndrome-associated germline succinate dehydrogenase complex subunit D (SDHD) variants cause PTEN-mediated down-regulation of autophagy in thyroid cancer cells. *Hum Mol Genet*. 2017;26:1365–1375.

205. Kimura F, Ueda A, Sato E, et al. Hereditary breast cancer associated with Cowden syndrome-related PTEN mutation with Lhermitte-Duclos disease. *Surg Case Rep*. 2017;3:83.

206. Chen XY, Lu F, Wang YM, et al. PTEN inactivation by germline/somatic c.950_953delTACT mutation in patients with Lhermitte-Duclos disease manifesting progressive phenotypes. *Clin Genet*. 2014;86:349–354.

207. Chen HJ, Romigh T, Sesock K, et al. Characterization of cryptic splicing in germline PTEN intronic variants in Cowden syndrome. *Hum Mutat*. 2017;38:1372–1377.

208. Bhargava R, Au Yong KJ, Leonard N. Bannayan-Riley-Ruvalcaba syndrome: MRI neuroimaging features in a series of 7 patients. *AJNR Am J Neuroradiol*. 2014;35:402–406.

209. Busa T, Milh M, Degardin N, et al. Clinical presentation of PTEN mutations in childhood in the absence of family history of Cowden syndrome. *Eur J Paediatr Neurol*. 2015;19:188–192.

210. Pritchard CC, Smith C, Marushchak T, et al. A mosaic PTEN mutation causing Cowden syndrome identified by deep sequencing. *Genet Med*. 2013;15:1004–1007.

211. Ngeow J, Eng C. Germline PTEN Mutation Analysis for PTEN Hamartoma Tumor Syndrome. *Methods Mol Biol*. 2016;1388:63–73.

212. Pilarski R, Burt R, Kohlman W, et al. Cowden syndrome and the PTEN hamartoma tumor syndrome: systematic review and revised diagnostic criteria. *J Natl Cancer Inst*. 2013;105:1607–1616.

213. Colby S, Yehia L, Niazi F, et al. Exome sequencing reveals germline gain-of-function EGFR mutation in an adult with Lhermitte-Duclos disease. *Cold Spring Harb Mol Case Stud*. 2016;2:a001230.

214. Nose V. Genodermatosis affecting the skin and mucosa of the head and neck: clinicopathologic, genetic, and molecular aspect—PTEN-hamartoma tumor syndrome/Cowden syndrome. *Head Neck Pathol*. 2016;10:131–138.

215. Romano C, Schepis C. PTEN gene: a model for genetic diseases in dermatology. *ScientificWorldJournal*. 2012;2012:252457.

216. Iskandarli M, Yaman B, Aslan A. A case of Bannayan-Riley-Ruvalcaba syndrome. A new clinical finding and brief review. *Int J Dermatol*. 2016;55:1040–1043.

217. Lok C, Viseux V, Avril MF, et al. Brain magnetic resonance imaging in patients with Cowden syndrome. *Medicine (Baltimore)*. 2005;84:129–136.

218. Wei G, Zhang W, Li Q, et al. Magnetic resonance characteristics of adult-onset Lhermitte-Duclos disease: an indicator for active cancer surveillance? *Mol Clin Oncol*. 2014;2:415–420.

219. Toelle S, Poretti A, Scheer I, et al. Bannayan-Riley-Ruvalcaba syndrome with progressive spinal epidural lipomatosis. *Neuropediatrics*. 2012;43:221–224.

220. Lee SH, Ryoo E, Tchah H. Bannayan-Riley-Ruvalcaba syndrome in a patient with a PTEN mutation identified by chromosomal microarray analysis: a case report. *Pediatr Gastroenterol Hepatol Nutr*. 2017;20:65–70.

221. Soysal Y, Acun T, Lourenco C, et al. Muscle hemangiomatosis presenting as a severe feature in a patient with the PTEN mutation: expanding the phenotype of vascular malformations in bannayan-riley-ruvalcaba syndrome. *Balkan J Med Genet*. 2012;15:45–50.

222. Moon K, Ducruet AF, Crowley RW, et al. Complex dural arteriovenous fistula in Bannayan-Riley-Ruvalcaba syndrome. *J Neurosurg Pediatr*. 2013;12:87–92.

223. Gunawan P, Lusiana L, Saharso D. Hemispherectomy procedure in Proteus syndrome. *Iran J Child Neurol*. 2016;10:86–90.

224. Biesecker L. The challenges of Proteus syndrome: diagnosis and management. *Eur J Hum Genet*. 2006;14:1151–1157.

225. Biesecker LG, Sapp JC. Proteus Syndrome. In: Adam MP, Ardinger HH, Pagon RA, et al., eds. *GeneReviews((R))*. Seattle, WA: University of Washington, Seattle University of Washington, Seattle; 1993GeneReviews is a registered trademark of the University of Washington, Seattle. All rights reserved.

226. Cohen Jr MM. Proteus syndrome review: molecular, clinical, and pathologic features. *Clin Genet*. 2014;85:111–119.

227. Li Z, Shen J, Liang J. Thoracolumbar scoliosis in a patient with Proteus syndrome: a case report and literature review. *Medicine (Baltimore)*. 2015;94:e360.

228. Happle R. Elattoproteus syndrome: delineation of an inverse form of Proteus syndrome. *Am J Med Genet*. 1999;84:25–28.

229. Valera MC, Vaysse F, Bieth E, et al. Proteus syndrome: report of a case with AKT1 mutation in a dental cyst. *Eur J Med Genet*. 2015;58:300–304.

230. Lindhurst MJ, Sapp JC, Teer JK, et al. A mosaic activating mutation in AKT1 associated with the Proteus syndrome. *N Engl J Med*. 2011;365:611–619.

231. Yamamoto A, Kikuchi Y, Yuzurihara M, et al. A case of Proteus syndrome with severe spinal canal stenosis, scoliosis, and thoracic deformity associated with tethered cord. *Jpn J Radiol*. 2012;30:336–339.